



**HAL**  
open science

# HBV Bypasses the Innate Immune Response and Does Not Protect HCV From Antiviral Activity of Interferon

Pascal Mutz, Philippe Metz, Florian A. Lempp, Silke Bender, Bingqian Qu, Katrin Schoneweis, Sefan Seitz, Thomas Tu, Agnese Restuccia, Jamie Frankish, et al.

► **To cite this version:**

Pascal Mutz, Philippe Metz, Florian A. Lempp, Silke Bender, Bingqian Qu, et al.. HBV Bypasses the Innate Immune Response and Does Not Protect HCV From Antiviral Activity of Interferon. *Gastroenterology*, 2018, 154 (6), pp.1791-1804. 10.1053/j.gastro.2018.01.044 . hal-02441618

**HAL Id: hal-02441618**

**<https://hal.science/hal-02441618>**

Submitted on 7 Mar 2022

**HAL** is a multi-disciplinary open access archive for the deposit and dissemination of scientific research documents, whether they are published or not. The documents may come from teaching and research institutions in France or abroad, or from public or private research centers.

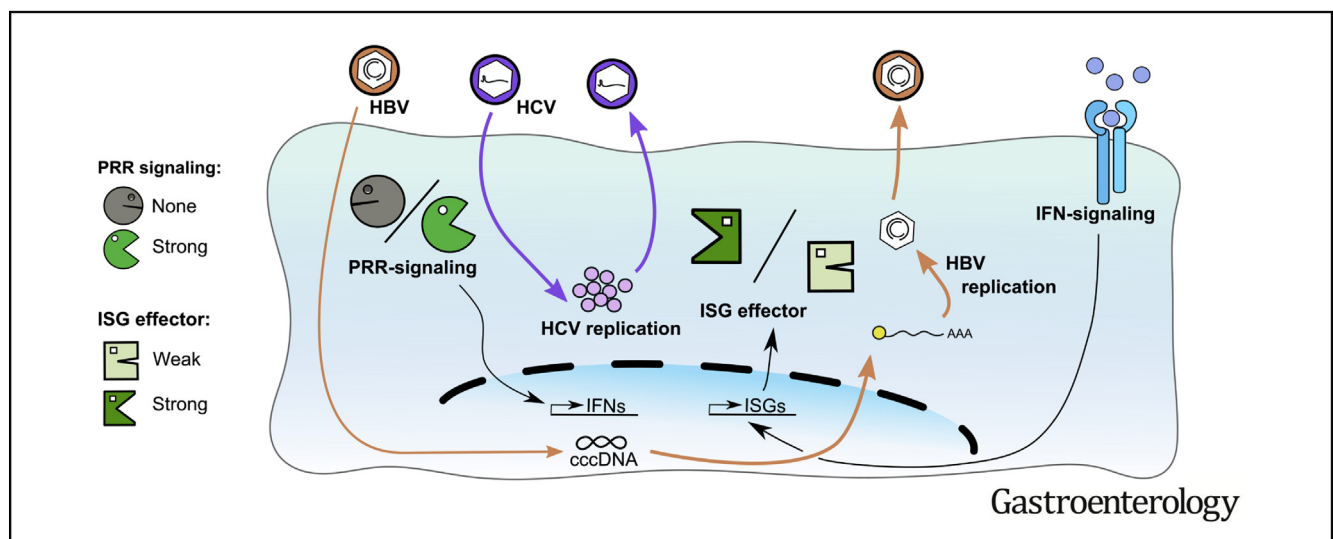
L'archive ouverte pluridisciplinaire **HAL**, est destinée au dépôt et à la diffusion de documents scientifiques de niveau recherche, publiés ou non, émanant des établissements d'enseignement et de recherche français ou étrangers, des laboratoires publics ou privés.



# HBV Bypasses the Innate Immune Response and Does Not Protect HCV From Antiviral Activity of Interferon

Pascal Mutz,<sup>1,2,3</sup> Philippe Metz,<sup>1</sup> Florian A. Lempp,<sup>1,4</sup> Silke Bender,<sup>1,2</sup> Bingqian Qu,<sup>1</sup> Katrin Schöneweis,<sup>1,4</sup> Stefan Seitz,<sup>1</sup> Thomas Tu,<sup>1</sup> Agnese Restuccia,<sup>1,2</sup> Jamie Frankish,<sup>5</sup> Christopher Dächert,<sup>5</sup> Benjamin Schusser,<sup>6</sup> Ronald Koschny,<sup>7</sup> Georgios Polychronidis,<sup>8</sup> Peter Schemmer,<sup>8,10</sup> Katrin Hoffmann,<sup>8</sup> Thomas F. Baumert,<sup>9</sup> Marco Binder,<sup>1,5</sup> Stephan Urban,<sup>1,4</sup> and Ralf Bartenschlager<sup>1,2,3,4</sup>

<sup>1</sup>Department of Infectious Diseases, Molecular Virology, Heidelberg University, Heidelberg, Germany; <sup>2</sup>Division of Virus-Associated Carcinogenesis (F170), German Cancer Research Center (DKFZ), Heidelberg, Germany; <sup>3</sup>HBIGS graduate school, Heidelberg, Germany; <sup>4</sup>German Centre for Infection Research (DZIF), partner site Heidelberg, Heidelberg, Germany; <sup>5</sup>Research Group “Dynamics of early viral infection and the innate antiviral response”, Division Virus-associated carcinogenesis (F170), German Cancer Research Center (DKFZ), Heidelberg, Germany; <sup>6</sup>Reproductive Biotechnology, School of Life Sciences Weihenstephan, Technical University of Munich, Munich, Germany; <sup>7</sup>Department of Gastroenterology, Infection and Intoxication, University Hospital Heidelberg, Heidelberg, Germany; <sup>8</sup>Department of General-, Visceral- and Transplant Surgery, University Hospital Heidelberg, Heidelberg, Germany; and <sup>9</sup>Inserm, U1110, Institut de Recherche sur les Maladies Virales et Hépatiques, Université de Strasbourg, Institut Hospitalo-Universitaire, Pôle Hépatodigestif, Nouvel Hôpital Civil, Strasbourg, France; <sup>10</sup>Division of Transplant Surgery, Medical University of Graz, Graz, Austria



**BACKGROUND & AIMS:** Hepatitis C virus (HCV) infection is sensitive to interferon (IFN)-based therapy, whereas hepatitis B virus (HBV) infection is not. It is unclear whether HBV escapes detection by the IFN-mediated immune response or actively suppresses it. Moreover, little is known on how HBV and HCV influence each other in coinfecting cells. We investigated interactions between HBV and the IFN-mediated immune response using HepaRG cells and primary human hepatocytes (PHHs). We analyzed the effects of HBV on HCV replication, and vice versa, at the single-cell level. **METHODS:** PHHs were isolated from liver resection tissues from HBV-, HCV-, and human immunodeficiency virus-negative patients. Differentiated HepaRG cells overexpressing the HBV receptor sodium taurocholate cotransporting polypeptide (dHepaRGNTCP) and PHHs were infected with HBV. Huh7.5 cells were transfected

with circular HBV DNA genomes resembling viral covalently closed circular DNA (cccDNA), and subsequently infected with HCV; this served as a model of HBV and HCV coinfection. Cells were incubated with IFN inducers, or IFNs, and antiviral response and viral replication were analyzed by immune fluorescence, reverse-transcription quantitative polymerase chain reaction, enzyme-linked immunosorbent assays, and flow cytometry. **RESULTS:** HBV infection of dHepaRGNTCP cells and PHHs neither activated nor inhibited signaling via pattern recognition receptors. Incubation of dHepaRGNTCP cells and PHHs with IFN had little effect on HBV replication or levels of cccDNA. HBV infection of these cells did not inhibit JAK-STAT signaling or up-regulation of IFN-stimulated genes. In coinfecting cells, HBV did not prevent IFN-induced suppression of HCV replication. **CONCLUSIONS:** In dHepaRGNTCP cells and

## EDITOR'S NOTES

## BACKGROUND AND CONTEXT

Unlike HBV infection, Hepatitis C virus (HCV) infection is sensitive to interferon (IFN)-based therapy. It is unclear whether HBV escapes detection by, or suppresses, the IFN-mediated immune response, and how HBV and HCV influence each other in co-infected cells.

## NEW FINDINGS

HBV neither activates nor inhibits the IFN response and is rather insensitive to IFN-induced antiviral state. HBV is a paradigm for a virus bypassing this important early antiviral defense system.

## LIMITATIONS

This study is based on the most advanced cell culture systems that are suitable to study the interplay between the IFN response and HBV as well as HCV.

## IMPACT

These results validate the concept of HBV passively bypassing the IFN system at every step of its replication cycle.

PHHs, HBV evades the induction of IFN and IFN-induced antiviral effects. HBV infection does not rescue HCV from the IFN-mediated response.

**Keywords:** Coinfection; Interferon-stimulated Gene; PRR; RIG-I.


With approximately 230 million chronically infected humans worldwide,<sup>1</sup> Hepatitis B virus (HBV) and Hepatitis C virus (HCV) are global health threats. Infections with either virus can lead to fibrosis, liver cirrhosis, and hepatocellular carcinoma (HCC).<sup>2</sup> HBV/HCV coinfecting individuals show faster disease progression and have higher HCC risk than mono-infected individuals.<sup>3</sup> Although both viruses share hepatotropism, their replication cycles and biological properties differ profoundly. HCV belongs to the family Flaviviridae and has a single-stranded RNA genome of positive polarity. HCV is capable of blocking innate immune signaling on several levels (eg, Mitochondrial antiviral-signaling protein cleavage by the nonstructural protein [NS]3-4A protease<sup>4</sup>), yet induces a strong interferon (IFN) response in primary human hepatocytes (PHH),<sup>5</sup> chimpanzees,<sup>6</sup> and acutely infected patients.<sup>7</sup> Nevertheless, HCV is highly sensitive to IFN- $\alpha$  treatment both in vitro<sup>8</sup> and in infected patients.<sup>9</sup>

Like HCV, HBV particles are enveloped but contain a partially double-stranded, circular DNA genome within their nucleocapsid. In infected cells, this genome is converted into episomal covalently closed circular DNA (cccDNA)<sup>10</sup> serving as persistence reservoir. In contrast to HCV, the way HBV interacts with the IFN system is only partially understood (reviewed in Faure-Dupuy et al<sup>11</sup>). This is due, at least in part, to the only recent discovery of the HBV receptor sodium taurocholate cotransporting polypeptide (NTCP)<sup>12</sup> enabling the establishment of widely

available infection systems. With respect to the IFN system, HBV is regarded as “stealth” virus, that is, it does not induce an IFN response as observed in chimpanzees,<sup>13</sup> acutely infected patients,<sup>14,15</sup> and some in vitro infection experiments.<sup>16,17</sup> However, an IFN- $\lambda$  response in induced hepatocyte-like cells derived from pluripotent stem cells<sup>18</sup> and a moderate up-regulation of IFN and IFN-stimulated genes (ISGs) in HBV-infected uPA/SCID mice repopulated with PHH have been reported.<sup>19</sup> Moreover, several groups found HBV proteins such as the HBx protein or the viral polymerase to actively block pattern recognition receptor (PRR)-mediated innate immune induction.<sup>20,21</sup> However, because these results are mainly based on artificial over-expression of HBV proteins, the physiological relevance remains elusive. Interestingly, Luangsay and colleagues<sup>22</sup> reported an inhibition of IFN induction by unknown factor(s) present in their HBV inoculum, whereas Lebossé et al<sup>23</sup> reported a down-regulation of selected, among others, innate immune genes in the liver of patients with chronic hepatitis B (CHB) that was, however, not correlated with HBV replication.

Equally controversial is the IFN sensitivity of HBV. On the one hand, only a minor proportion of patients with CHB can eliminate the virus by pegylated IFN treatment,<sup>24</sup> consistent with results from various infection models in which HBV replication can be reduced, but not eliminated, by IFN treatment.<sup>25</sup> Moreover, several studies report a difference in IFN sensitivity of different HBV genotypes,<sup>26</sup> but this could not be recapitulated in cell culture.<sup>27</sup> On the other hand, stable HBV integrations are nearly nonresponsive to IFN treatment unless supraphysiological amounts of IFN are used,<sup>28</sup> arguing that HBV might directly counteract IFN signaling (eg, by modifying the transcription factor STAT1 [Signal transducer and activator of transcription]).<sup>29,30</sup> In contrast, in HBV/HCV coinfecting patients, HCV can be controlled by IFN both in co- and in mono-infected patients,<sup>31</sup> and in an engineered HBV/HCV cell culture system, viral interference was not found.<sup>32</sup>

**Abbreviations used in this paper:** APOBEC, apolipoprotein B mRNA editing enzyme catalytic subunit; cccDNA, covalently closed circular DNA; CHB, chronic hepatitis B; circDNA, circular DNA; GFP-IRF3, green fluorescent protein–interferon regulatory factor 3; HBeAg, hepatitis B e antigen; HBsAg, hepatitis B surface antigen; HBV, hepatitis B virus; HCV, hepatitis C virus; dHepaRG<sup>NTCP</sup>, differentiated HepaRG stably expressing NTCP; IFN, interferon; ISG, IFN-stimulated gene; MDA5, Melanoma Differentiation-Associated protein 5; Mengo<sup>Zn</sup>, Mengovirus zinc mutant; Mx1, Interferon-induced GTP-binding protein Mx1; NF- $\kappa$ B, nuclear factor ‘kappa-light-chain-enhancer’ of activated B-cells; NS, nonstructural protein; NTCP, sodium taurocholate cotransporting polypeptide; PBS, phosphate-buffered saline; pgRNA, pregenomic RNA; PHH, primary human hepatocytes; p.i., postinfection; (p)STAT, (phospho) Signal transducer and activator of transcription; PRR, pathogen recognition receptor; qPCR, quantitative polymerase chain reaction; RIG-I, retinoic acid-inducible gene 1; RVFV, Rift valley fever virus; STING, Stimulator of interferon genes; TLR3, Toll-like receptor 3.

 Most current article

© 2018 by the AGA Institute. Published by Elsevier Inc. This is an open access article under the CC BY-NC-ND license (<http://creativecommons.org/licenses/by-nc-nd/4.0/>).

0016-5085

<https://doi.org/10.1053/j.gastro.2018.01.044>

Here we investigated the interplay of HBV and the IFN system in an immune-competent infection system in which HBV replication is driven from cccDNA. We used differentiated and fully permissive HepaRG cells ectopically expressing NTCP (dHepaRG<sup>NTCP</sup>),<sup>33</sup> as well as PHH, and characterized HBV-infected cells on a single-cell level. We also studied the interaction of HBV and HCV with the IFN system by using a newly established immune-competent HBV/HCV coreplication system.

## Material and Methods

Unless specified, detailed information about used materials and methods can be found in the [supplementary material and methods](#) section.

### Primary Human Hepatocyte Isolation

PHH for experiments in [Figure 1](#) and [Supplementary Figure 1](#) were isolated from liver resections of HBV-, HCV-, and human immunodeficiency virus-negative patients. All patients gave written informed consent for the experimental use of their resected liver tissue. Ethical approval is covered with German reference number #S-161/2007. PHH isolation was performed as described previously.<sup>34</sup> Cells were seeded at a density of approximately  $7 \times 10^5$  cells/mL on rat tail collagen (Collagen R, #47254; Serva, Heidelberg, Germany) coated plates and cultured in Williams E medium containing 1.5% dimethyl sulfoxide, 100  $\mu$ g/mL Gentamicin (Life Technology, Darmstadt, Germany), 82.56 mM hydrocortisone buffered with 10 mM Hepes [pH 7.4], 0.09  $\mu$ g/mL insulin, 28.7 mL/ 500 mL medium PDH mix (1.12 mM glutamax; Gibco, Waltham, MA, 6 mL 5% glucose, 11.5 mL 1 M Hepes [pH 7.4], 112 U/mL penicillin/ streptomycin [#15140-22, Life Technology]). PHH used for experiments shown in [Supplementary Figure 7](#) were cryopreserved and kindly provided by T. Baumert. PHH used for the experiments shown in [Supplementary Figures 12](#) and [13](#) were obtained from Biopredic (St Gregoire, France) and Cytes (Barcelona, Spain).

### Immunofluorescence and Image Analysis

Cells were fixed with 4% paraformaldehyde in phosphate-buffered saline (PBS) for 10 minutes and permeabilized with 0.5% Triton X-100 in PBS for 10 minutes. For phospho-STAT1 (pSTAT1) images, cells were fixed and permeabilized with ice cold methanol for 20 minutes at  $-20^\circ\text{C}$ . All samples were incubated for 1 hour with 3% bovine serum albumin in PBS and stained with the primary antibody ([Supplementary Table 1](#)), diluted in PBS/1% bovine serum albumin, overnight at  $4^\circ\text{C}$ . Cells were washed thrice with PBS and incubated for 1 hour with the respective secondary antibody ([Supplementary Table 2](#)). Nuclear DNA was stained with DAPI (4',6-diamidino-2-phenylindole; MoBiTec, Gottingen, Germany). Cover slides were mounted with fluoromount G (SouthernBiotech, Birmingham, AL). Image acquisition was performed with a Nikon (Tokyo, Japan) eclipse Ti microscope followed by image processing with ImageJ (National Institutes of Health, Bethesda, MD). Images from one experiment were processed the same way. The Ilastik software package (open source, version 1.3.0, [ilastik.org](http://ilastik.org); Heidelberg, Germany)<sup>35</sup> was used to determine translocation events for green fluorescent protein-interferon regulatory factor 3 (GFP-IRF3) and

endogenous nuclear factor "kappa-light-chain-enhancer" of activated B-cells (NF- $\kappa$ B).

### Statistics

All statistical analyses were performed using the Prism software package version 6 (GraphPad Software, Inc., La Jolla, CA). Unpaired Student *t* test was used to determine statistical significance. Paired Student *t* test was performed when groups of the same sample were compared (always indicated as "same sample" in the figure). Significance levels are indicated by asterisks: \**P* < .05; \*\**P* < .01; \*\*\**P* < .001; ns, not significant.

## Results

### HBV Replicates in Immune-Competent Differentiated HepaRG<sup>NTCP</sup> Cells and PHHs and Bypasses the Intracellular PRRs RIG-I, MDA5, and TLR3

To investigate whether HBV can induce an IFN response at any step of the viral life cycle, we infected immune-competent dHepaRG<sup>NTCP</sup> and PHH with HBV (genotype D). The entry inhibitor Myrcludex B<sup>33</sup> added during inoculation served as control to rule out unspecific IFN induction by residual components contained in the virus stock. Infection efficiency was approximately 5% in case of dHepaRG<sup>NTCP</sup> cells and >90% in case of PHH as determined by HBV core-specific immunofluorescence ([Figure 1A](#)). To monitor HBV replication kinetics, total RNA was harvested at several time points after infection and pregenomic RNA (pgRNA) was quantified by reverse-transcriptase quantitative polymerase chain reaction (qPCR). pgRNA abundance reached a plateau in both cell types 4 days after infection ([Figure 1B](#)), similar to the production kinetics of hepatitis B e antigen (HBeAg) and hepatitis B surface antigen (HBsAg) ([Figure 1C](#)). Entry inhibition by Myrcludex B reduced replication markers 10- to 100-fold.

Although HBV could infect both cell lines and replicate with similar kinetics, no IFN- $\lambda$ 1 or IFN- $\beta$  induction was detected with  $C_t$  values in the background range ([Figure 1D](#)). Consistently, mRNA levels of multiple ISGs selected on the basis of the study by Lebossé et al.<sup>23</sup> did not change after HBV infection ([Supplementary Figure 1A](#) and [B](#)), corroborating the lack of IFN response activation. This was not due to IFN deficiency of used cells as revealed by the up-regulation of IFN and ISGs on stimulation of naïve dHepaRG<sup>NTCP</sup> or PHH with Sendai virus or Rift valley fever virus  $\Delta$ NSs (RVFV), 2 activators of the retinoic acid-inducible gene 1 (RIG-I) pathway,<sup>36,37</sup> or with the Mengovirus zinc mutant (Mengo<sup>Zn</sup>), a profound inducer of the Melanoma Differentiation-Associated protein 5 (MDA5) pathway.<sup>36</sup> Moreover, also poly(I:C) added into the culture supernatant to trigger the Toll-like receptor 3 (TLR3) pathway<sup>38,39</sup> induced the expression of IFNs and ISGs up to 1000-fold ([Supplementary Figure 1C](#)).

We corroborated this result in dHepaRG<sup>NTCP</sup> cells with another HBV genotype (C2) being highly prevalent in Asia<sup>40</sup> and reported recently to induce an IFN response.<sup>41</sup>

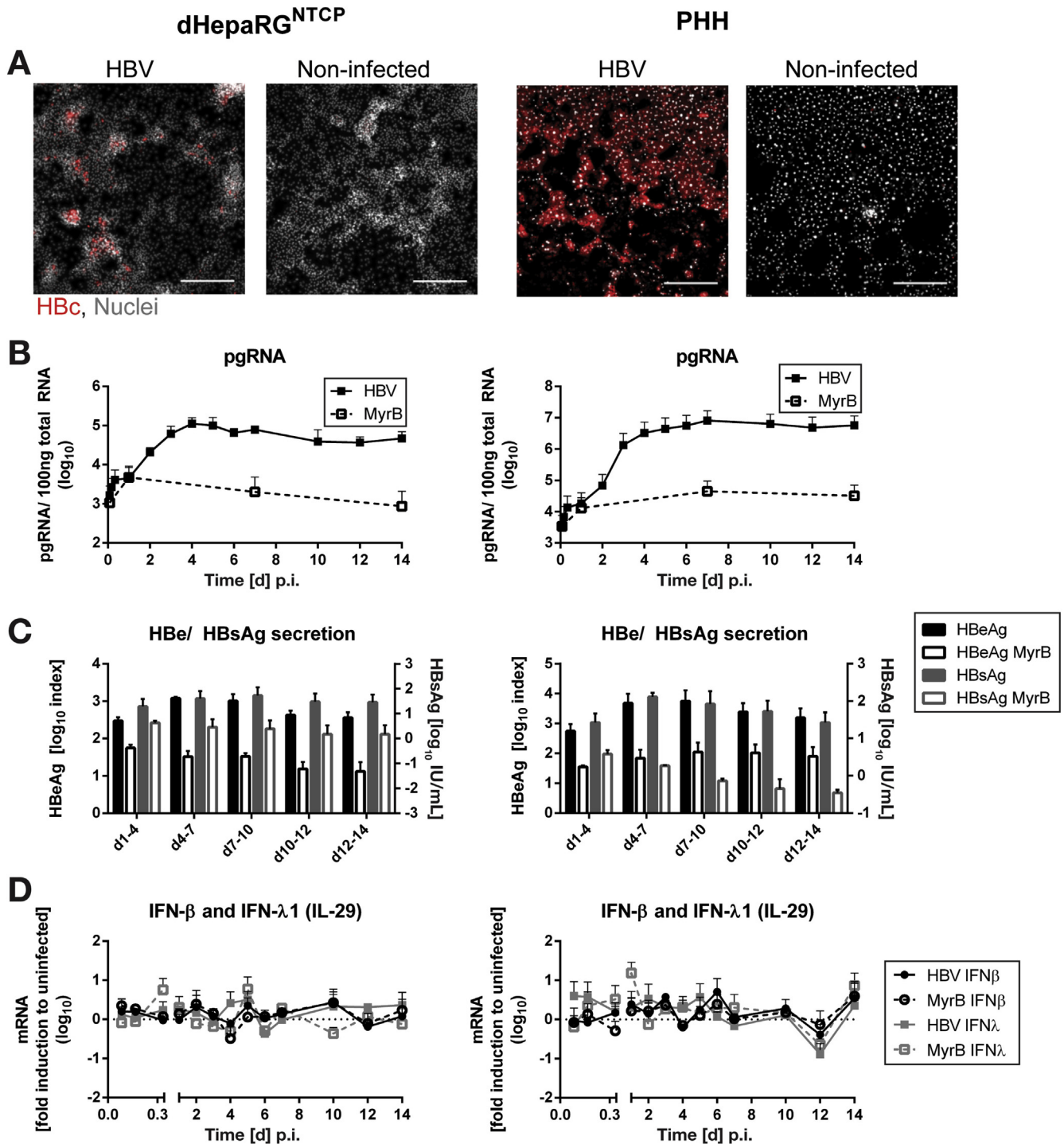


**Figure 1.** Robust infection of dHepaRG<sup>NTCP</sup> cells and PHHs with HBV does not induce an interferon response. Differentiated HepaRG<sup>NTCP</sup> cells or PHHs were infected with HBV genotype D (multiplicity of infection = 100 genome equivalents/cell). (A) Fourteen days p.i., infection efficiency was determined by staining for viral core protein (red). Nuclear DNA was stained with DAPI (gray). Scale bar = 300  $\mu$ m. (B) Time course of pgRNA accumulation in HBV-infected cells. (C) Kinetics of HBeAg and HBsAg secretion. (D) IFN- $\beta$  and IFN- $\lambda$ 1 mRNA abundance was determined by reverse-transcriptase qPCR at indicated time points. Early time points are 2, 4, and 8 hours p.i. Myrcludex B (200 nM) served as HBV entry inhibitor control in (B) to (D). Values are means and SDs from 2 independent experiments.

Replication of this isolate was well detectable, although somewhat lower than the genotype D strain (Supplementary Figure 2A and B), but did not induce an IFN response either (Supplementary Figure 2C and D). Thus, HBV either avoids

activation of the IFN pathways or effectively suppresses them, in any case independent from the genotype.

To distinguish between passive or active evasion, we monitored nuclear translocation of NF- $\kappa$ B and IRF3, key

events in the early activation of the cytokine response. For this and all subsequent experiments, owing to higher replication, we used HBV genotype D. Although detection of endogenous NF- $\kappa$ B by immunofluorescence was well possible, endogenous IRF3 levels could not be visualized unambiguously with available antibodies. Therefore, we established dHepaRG<sup>NTCP</sup> cells stably expressing GFP-tagged IRF3 (dHepaRG<sup>NTCP</sup> GFP-IRF3) to monitor at single-cell level IRF3 translocation. Notably, expression of the GFP-IRF3 reporter did not affect HBV replication, qualifying this cell system for our analysis (Supplementary Figure 3). To monitor whether HBV was capable of blocking RIG-I, MDA5, or TLR3-mediated signaling, we infected dHepaRG<sup>NTCP</sup> GFP-IRF3 cells with HBV. Several days later (ie, when HBV replication was robustly established), cells were stimulated as described in Figure 2 to activate the signaling pathways. NF- $\kappa$ B did not translocate into the nucleus both in nonstimulated, HBV-negative cells, and in HBV-infected cells (Figure 2A). This was not due to an activation block, because NF- $\kappa$ B translocation was well detected in HBV-infected cells stimulated with RVFV or Mengo<sup>Zn</sup> virus or poly(I:C) (Figure 2A and C; Supplementary Figures 4–6). Importantly, the extent of NF- $\kappa$ B nuclear translocation was comparable between HBV-positive and -negative cells (30%–50%) and also found in PHH (Supplementary Figure 7). Analogous results were found with nuclear translocation of GFP-IRF3 (Figure 2B and D; Supplementary Figures 4–6). Although a minor, but in the background range, nuclear translocation was found in HBV-infected cells in the absence of stimulation, the magnitude of GFP-IRF3 translocation in stimulated cells was well comparable between HBV-infected and noninfected cells.

To exclude that GFP-IRF3 and NF- $\kappa$ B translocation in HBV-infected cells is not induced by cytokines released from HBV-negative stimulated cells, but directly induced within the HBV-positive cell, we analyzed culture supernatants of RVFV or Mengo<sup>Zn</sup>-virus infected cells for the presence of activating cytokines. Supernatants were transferred onto nonstimulated cells and NF- $\kappa$ B or GFP-IRF3 nuclear translocation was monitored. Although tumor necrosis factor- $\alpha$  (used as control) induced NF- $\kappa$ B, but not GFP-IRF3 translocation, culture supernatants from stimulated cells did not (Supplementary Figure 8) supporting our conclusion that activation of NF- $\kappa$ B and GFP-IRF3 is induced within HBV-infected cells and not by cytokines released from bystander cells.

### HBV Is Only Moderately Sensitive Toward the IFN- $\alpha$ Induced Antiviral State

Having found that HBV did not block the IFN induction pathways, we next investigated whether HBV is sensitive toward ectopic IFN treatment. We treated dHepaRG<sup>NTCP</sup> cells with IFN- $\alpha$  as depicted schematically in Figure 3A. Consistent with a previous study,<sup>25</sup> the number of HBV-infected cells (Figure 3B), the levels of HBeAg and HBsAg secretion (Figure 3C and D) and pgRNA levels (Figure 3E) were reduced. Strongest effects were observed when cells were treated with IFN- $\alpha$  before HBV infection and throughout the observation period (condition “A”) reducing these markers to 20% to 30% of nontreated cells. Treating

the cells after virus inoculation for 9 days reduced viral markers to approximately 50% (condition “B”). Stopping treatment at day 4 postinfection (p.i.) or treating with IFN- $\alpha$  between day 4 and 10 p.i. had the lowest impact on HBV replication (condition “C” and “D,” respectively). Interestingly, cccDNA levels were not reduced by any of these treatment conditions as determined by qPCR or Southern blot (Figure 3F; Supplementary Figure 9, respectively), arguing for an IFN- $\alpha$  induced block of HBV replication predominantly at the level of transcription and/or RNA translation. Notably, IFN- $\alpha$  treatment neither impaired bile salt transport of NTCP, nor the ability of preS1-domain of the large HBV surface protein binding to NTCP, arguing against HBV entry inhibition (Supplementary Figure 10).

### HBV Does Not Block Jak-STAT Signaling and Subsequent ISG Expression

Given the very moderate inhibition of HBV by IFN- $\alpha$ , we explored if HBV could block IFN- $\alpha$ -mediated signaling by monitoring nuclear translocation of pSTAT1 and activation of ISG expression. We stimulated dHepaRG<sup>NTCP</sup> cells 8 days p.i. with HBV for 90 minutes with different concentrations of IFN- $\alpha$  and quantified nuclear translocation events by immunofluorescence microscopy. In untreated cells, virtually no nuclear pSTAT1 signal was detected, both in HBV-negative and HBV-positive cells (Figure 4A; Supplementary Figure 11). However, on IFN- $\alpha$  treatment, pSTAT1 translocation was observed in uninfected and HBV-infected cells, indicating that HBV does not block STAT1 phosphorylation and subsequent nuclear translocation. The percentage of cells with nuclear pSTAT1 signal increased to nearly 100% in an IFN concentration-dependent manner (Figure 4B). At any given IFN concentration, HBV did not block pSTAT1 translocation, but instead increased translocation at low IFN- $\alpha$  concentration with the number HBV-positive cells being twice as high on treatment with 10 IU/mL IFN- $\alpha$  (Figure 4B). Of note, comparable results were obtained with PHH (Supplementary Figure 12).

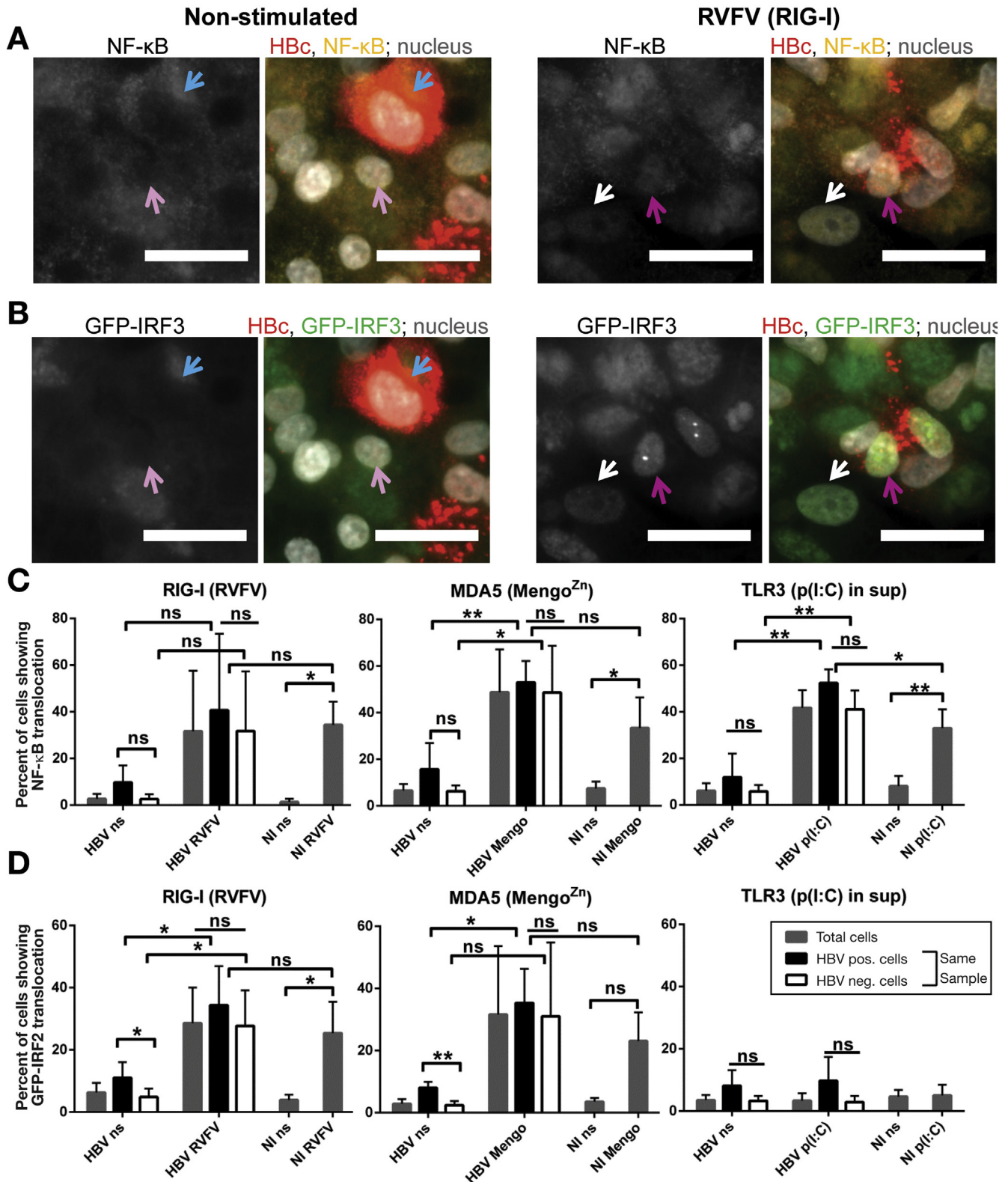
To examine whether translocated pSTAT1 induces ISG expression, we stimulated HBV-infected dHepaRG<sup>NTCP</sup> cells at day 7 p.i. for 24 hours with different concentrations of IFN- $\alpha$  and measured the expression of HBV core as well as the ISG Interferon-induced GTP-binding protein Mx1 (Mx1) by flow cytometry (Figure 4C). Mx1 was undetectable in most nonstimulated cells and independent from HBV. Expression of Mx1 increased dose dependently after IFN- $\alpha$  treatment in noninfected and HBV-infected cells, the latter reacting even more pronounced (Figure 4D). Analogous results were obtained with PHH examined by immunofluorescence microscopy (Supplementary Figure 13). Taken together, these results show that HBV does not counteract IFN- $\alpha$ -mediated ISG expression in fully permissive immune-competent cells.

### Transfected Circular HBV DNA Genomes Serve as cccDNA Surrogate and Allow HBV/HCV Coreplication in Huh7.5 Cells

Although rare, HBV/HCV coinfection profoundly increases the risk of serious liver damage as compared with

mono-infection. To study the impact of HBV/HCV coinfection on the IFN response, we took advantage of the fact that HCV is highly sensitive to IFN and, thus, a sensitive probe to monitor the antiviral state in a cell coreplicating HBV. Therefore, we established a system that is based on the use

of the highly HCV-permissive Huh7 cell clone Huh7.5.<sup>42</sup> Although these cells are poorly permissive for HBV entry, even on stable overexpression of NTCP, they support highly efficient HCV replication. This is not the case with HepG2<sup>NTCP</sup> and dHepaRG<sup>NTCP</sup>, as well as PHH where HCV



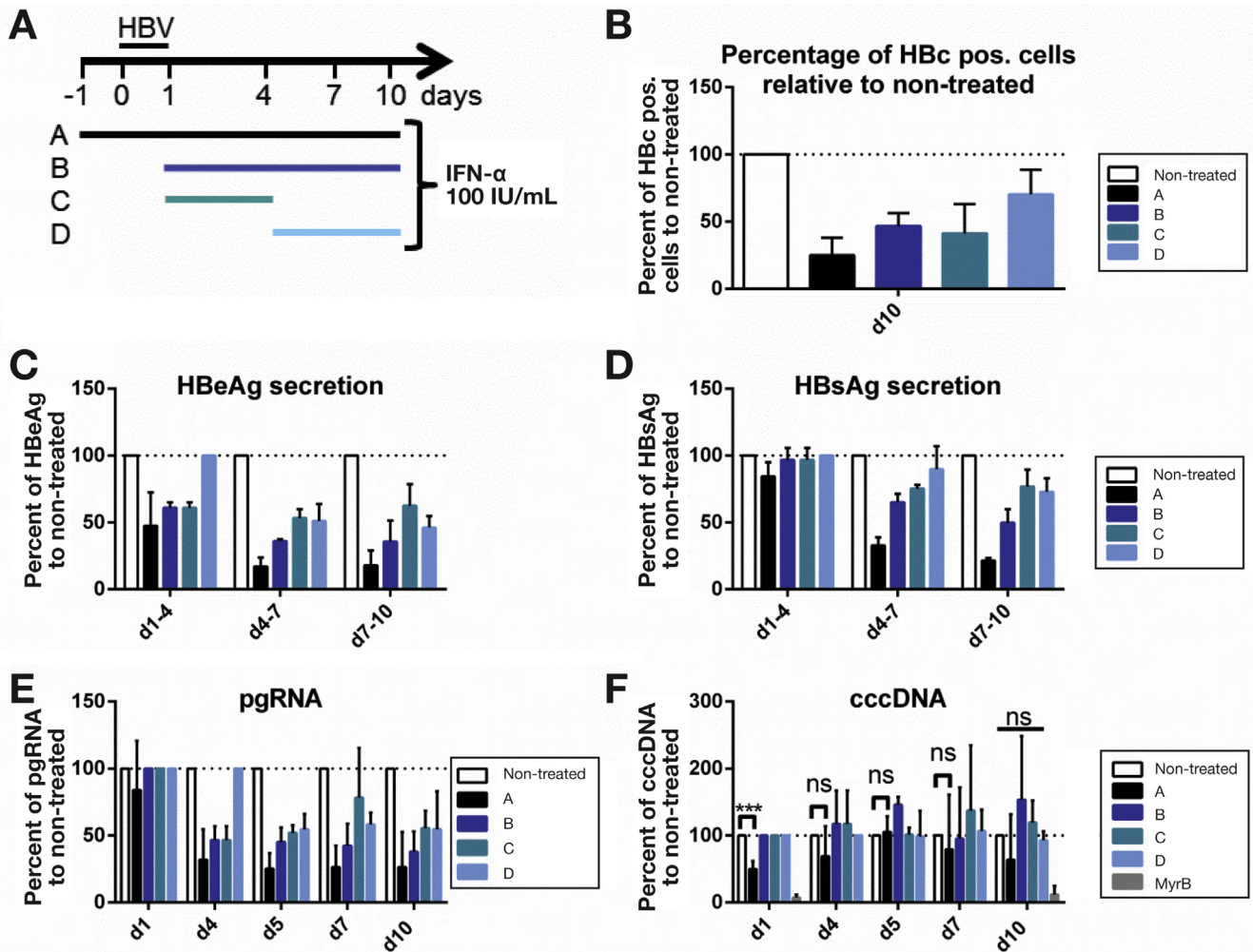


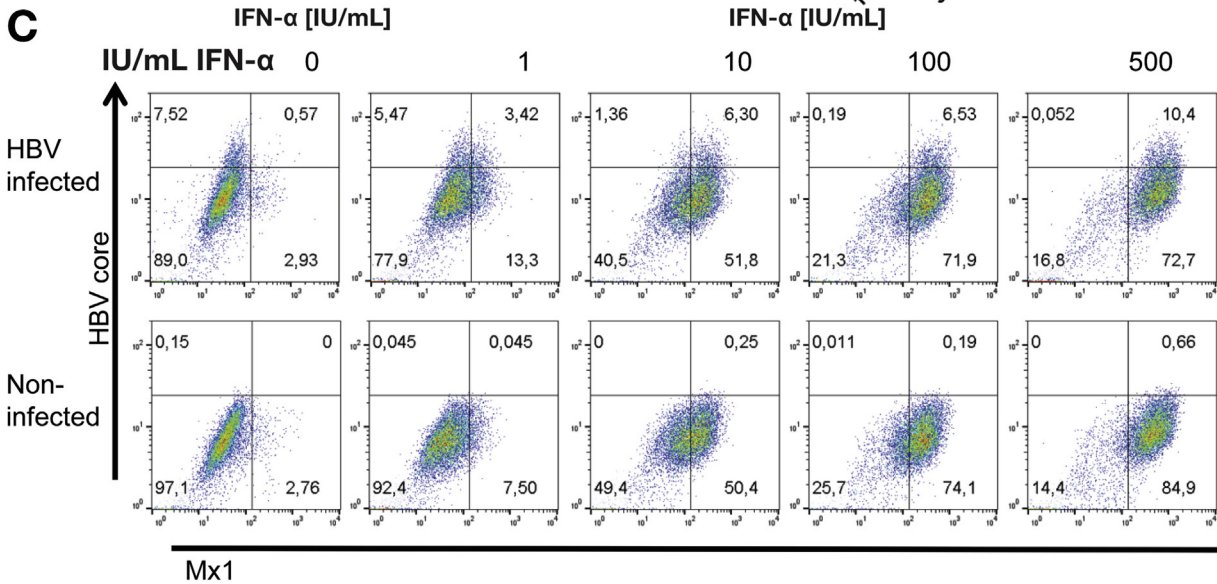
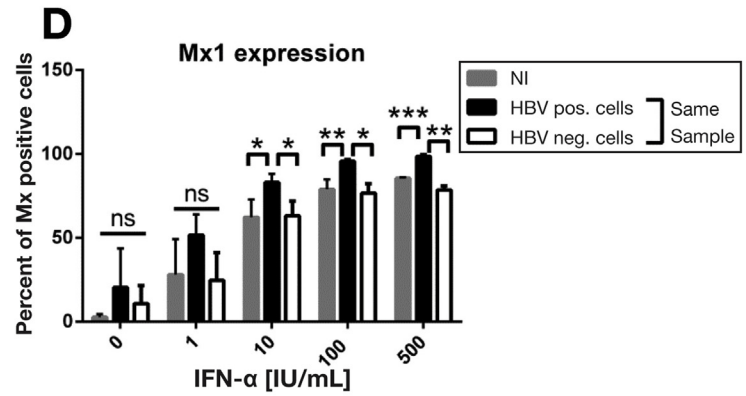
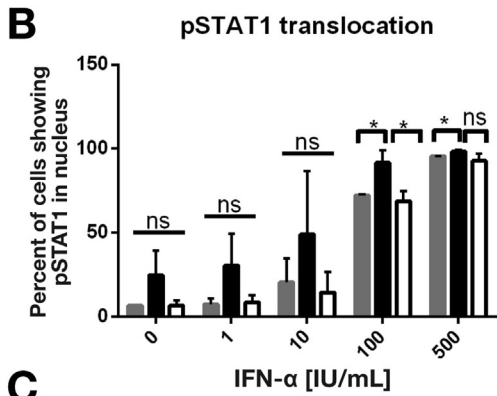
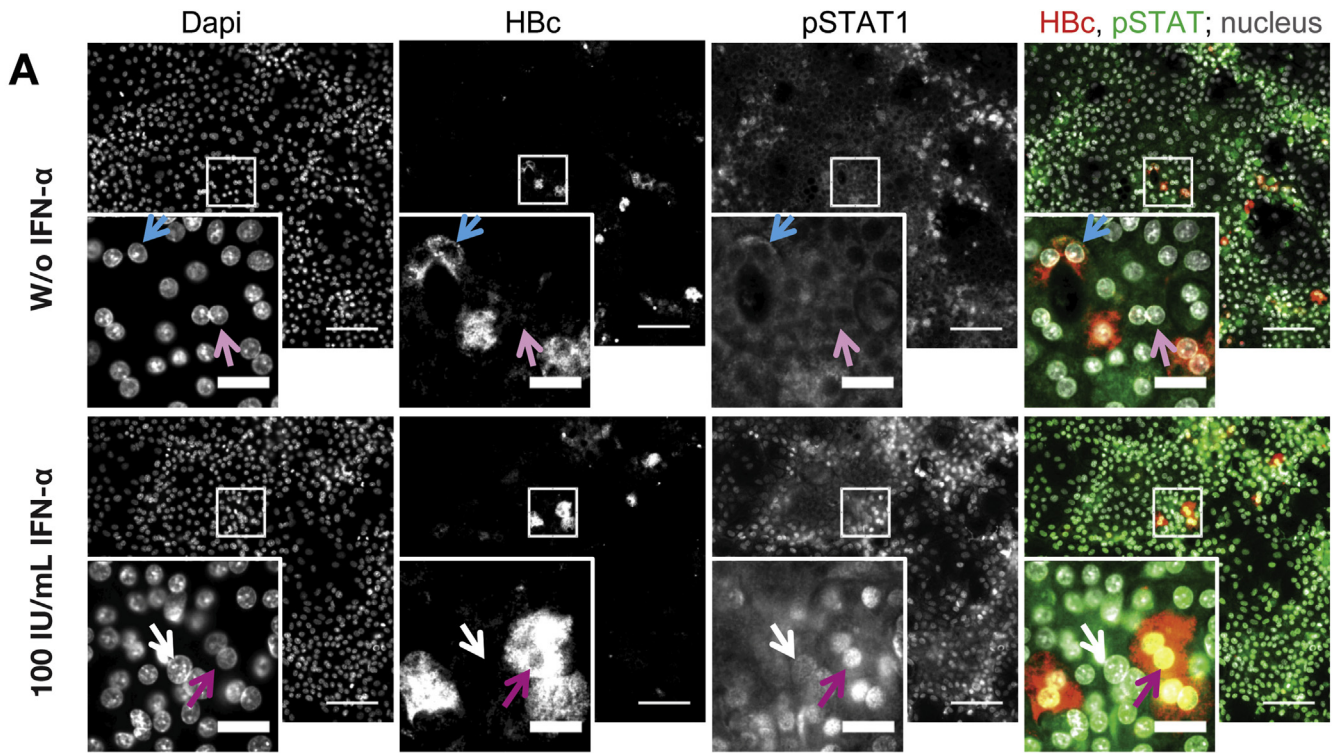
**Figure 3.** Limited inhibition of HBV replication by the antiviral state induced by IFN- $\alpha$ . dHepaRG<sup>NTCP</sup> cells were infected with HBV and treated with 100 IU/mL IFN- $\alpha$  at time points depicted in (A), or left untreated. The percentage of HBV core-positive cells at day 10 p.i. (B) as well as the kinetics of HBeAg and HBsAg secretion (C and D, respectively), pgRNA (E) and cccDNA accumulation (F) were quantified and normalized to the corresponding nontreated controls. Values obtained with cells treated with the entry inhibitor Myrcludex B (200 nM) added during HBV-inoculation served as negative control (day 1 and day 10 for cccDNA). n = 3 for all samples except for cccDNA (n = 4). HBV core-positive cells were determined by flow cytometry. \*\*\*P < .001; ns, not significant.

replication is very transient.<sup>5</sup> To overcome the limitation of Huh7.5 cells for HBV entry, we generated circular and authentic full-length HBV genomes by using in vitro ligation (Figure 5A). These genomes, designated here HBV circulating DNA (circDNA), lack any heterologous sequence and

on transfection into Huh7.5 cells served as a cccDNA surrogate.<sup>43,44</sup> Approximately 10% of the cells expressed HBV core protein 7 days after transfection (Figure 5B). HBeAg amounts released from transfected cells were stable throughout a 10-day observation period and slightly higher

**Figure 2.** Activation of RIG-I-, MDA5-, or TLR3-mediated signaling is not modulated by HBV in dHepaRG<sup>NTCP</sup> cells. HBV-infected dHepaRG<sup>NTCP</sup> GFP-IRF3 cells were stimulated at 7 days p.i. with RVFV $\Delta$ NSs (RIG-I inducer; 20x median effective concentration) for 16 hours, or at 8 days p.i. with the Mengo<sup>Zn</sup> virus (MDA5 inducer; multiplicity of infection = 10) for 8 hours, or at 8 days p.i. with 10  $\mu$ g/mL poly (I:C) added into the culture supernatant for 1 hour to stimulate the TLR3 pathway. (A and B) Representative zoomed images showing translocation of endogenous NF- $\kappa$ B (A) or GFP-IRF3 (B) in HBV-infected cells with or without RVFV $\Delta$ NSs stimulation. NF- $\kappa$ B is shown in yellow, HBV core in red, GFP-IRF3 in green, and nuclei in gray. Light blue arrows: HBV-infected cells without translocation; pink arrows: HBV-infected cells with NF- $\kappa$ B or GFP-IRF3 translocation; rosy arrows: noninfected cells without translocation; white arrows: noninfected cells with nuclear NF- $\kappa$ B or GFP-IRF3. Scale bar = 25  $\mu$ m. (C) Quantification of NF- $\kappa$ B translocation events in HBV- or noninfected (NI) cells that were either nonstimulated (ns) or stimulated by infection with RVFV $\Delta$ NSs or Mengo<sup>Zn</sup> or by treatment with p(I:C). (D) Quantification of GFP-IRF3 translocation events after treatment, as in (C). For (C) and (D): Images were quantified with the ILASTIC software package analyzing 8 to 10 images per condition and experiment from at least 3 independent experiments. Approximately 12,000 cells were analyzed per condition. \*P < .05; \*\*P < .01; ns, not significant.





than HBeAg amounts released from cells transfected with a control plasmid encoding an HBV overlength genome under control of a cytomegalovirus promoter (Figure 5C). Further, by using qPCR and subcellular fractionation, we calculated that one transfected cell contains approximately 300 copies of circHBV DNA (Supplementary Figure 14). Although this exceeds cccDNA levels observed in humans, circDNA abundance is similar to the one reported for other model systems (~50 copies/cell).<sup>10</sup>

To evaluate whether HBV-replicating cells can be superinfected with HCV, we infected Huh7.5 cells 4 days after transfection with HCV and quantified HBV core and HCV NS5A protein expression in single cells using flow cytometry 5 days after HCV infection (Figure 5D). We did not observe a correlation between HBV core and HCV NS5A levels in cells expressing both proteins arguing that replication of one virus does not affect replication of the other. Consistently, approximately 40% of both, the total and the HBV-positive, cell populations were infected by HCV (Figure 5E), and HCV did not affect HBV replication as deduced from the HBV core protein expression determined by flow cytometry (Figure 5D). Moreover, HBsAg amounts released from the cells were well comparable between HBV single-positive and HBV/HCV double-positive cells (Figure 5F). We concluded that HBV replication does not hamper HCV superinfection in Huh7.5 cells.

### HBV Does Not Protect HCV From the Antiviral Activity of IFN

Taking advantage of this cell culture system we investigated whether HBV suppresses the IFN response and protects HCV from the antiviral state induced by ectopically added IFN. HBV circDNA-transfected Huh7.5 cells were treated with 100 IU/mL IFN- $\alpha$  or 10 ng/mL IFN- $\lambda$ 1 one day before HCV superinfection ("pre"-treatment) or after superinfection ("post"-treatment) (Figure 6A). We chose these 2 IFN types because they play important roles in HCV<sup>6,45</sup> and used concentrations with comparable biological activity as determined with an HCV-based bio-assay (Supplementary Figure 15A). HBV was not affected by IFN treatment, whereas HCV was reduced by 80% (Figure 6B and C). Importantly, the number of HCV-positive cells was reduced to the same extent in HBV-negative and HBV-positive cells, demonstrating that HBV did not protect HCV from the antiviral state of IFN- $\alpha$  (Figure 6B and C) and IFN- $\lambda$  (Figure 6C and Supplementary Figure 15B). In summary, these results show that HBV does not interfere with IFN- $\alpha$

induced signaling and is unable to rescue HCV from the antiviral state induced by these cytokines.

## Discussion

By using single-cell analyses of dHepaRG<sup>NTCP</sup> cells and PHH we obtained results in full support of the concept that HBV is a "stealth" virus bypassing the IFN response. Consistent with that, Suslov and coworkers (personal communication, 2017) did not observe a PRR block by HBV after Sendai virus or poly(I:C) stimulation using liver biopsies obtained from patients with CHB. Moreover, very recently Cheng et al<sup>17</sup> also reported passive evasion of HBV from the innate immune system in hepatocytes.

Earlier studies described counteractions against PRR signaling (eg, mediated by HBx or the viral polymerase).<sup>20,21</sup> Moreover, several groups reported interference with IFN signaling by HBV.<sup>29,46,47</sup> These results are at variance with our report, but the studies were based on artificial overexpression of individual HBV proteins and, thus, their physiological relevance remains to be determined. Moreover, Sato and colleagues<sup>41</sup> reported an HBV genotype C-dependent activation of the IFN system, which we did not detect. The reasons for this discrepancy are unclear, but might be due to the experimental conditions used, such as the purification method of virus inocula. Likewise, Luangsay et al<sup>22</sup> reported an inhibition of PRR-mediated signaling by HBV, which they ascribe to an unknown component present in their HBV inoculum apparently absent in our virus preparation (Supplementary Figure 16). Alternatively, other PRRs and signaling pathways, such as cyclic GMP-AMP Synthase/Stimulator of interferon genes (STING) or IFI16 might be inhibited by HBV, as reported earlier by Liu and coworkers.<sup>21</sup> However, also the latter study was based on overexpression of a single HBV protein (the P-protein) and therefore, the in vivo relevance of the finding remains to be determined. In any case, we note that in many studies, including ours, only responses from hepatocytes were analyzed, whereas in vivo immune cells, such as T-cells, NK-cells, Kupffer cells, and others sense HBV infection.<sup>48</sup> This might explain why successful response to IFN therapy appears to correlate with the activation of distinct immune pathways.<sup>49</sup>

The mechanism by which HBV hides from PRR sensing most likely is due to its replication strategy. All viral RNAs are generated by cellular enzymes from the cccDNA and have a regular 5' cap and 3' poly(A) tail. The pgRNA is packaged into nucleocapsids and shielded from cytoplasmic

**Figure 4.** HBV does not block IFN- $\alpha$  mediated signaling and subsequent ISG expression. HBV-infected dHepaRG<sup>NTCP</sup> cells treated with given concentrations of IFN- $\alpha$  for 90 minutes at day 8 p.i. were harvested for pSTAT1 analysis (A and B) or treated for 24 hours with IFN- $\alpha$  at day 7 p.i. before Mx1 detection (C and D). (A) Representative immunofluorescence overview and zoom images (insets indicated by white squares) of HBV-infected cells mock treated or with 100 IU/mL IFN- $\alpha$ . Merge images show nuclear DNA (DAPI; gray), HBV core (red) and pSTAT1 (green). Light blue arrows: HBV-infected cells without pSTAT1 translocation; rosy arrows: noninfected cells without translocation; pink arrows: HBV-infected cells with pSTAT1 translocation; white arrows: noninfected cells with nuclear pSTAT1. Scale bars = 100  $\mu$ m and 25  $\mu$ m (overview and insert, respectively). (B) Quantification of 3 independent experiments of (A). (C) Representative panels of flow cytometry analysis of HBV core- (y-axis) and Mx1- (x-axis) expressing cells 24 hours after IFN- $\alpha$  treatment. (D) Quantification of 3 independent experiments of (C). ns, not significant; \* $P$  < .05; \*\* $P$  < .01; \*\*\* $P$  < .001.

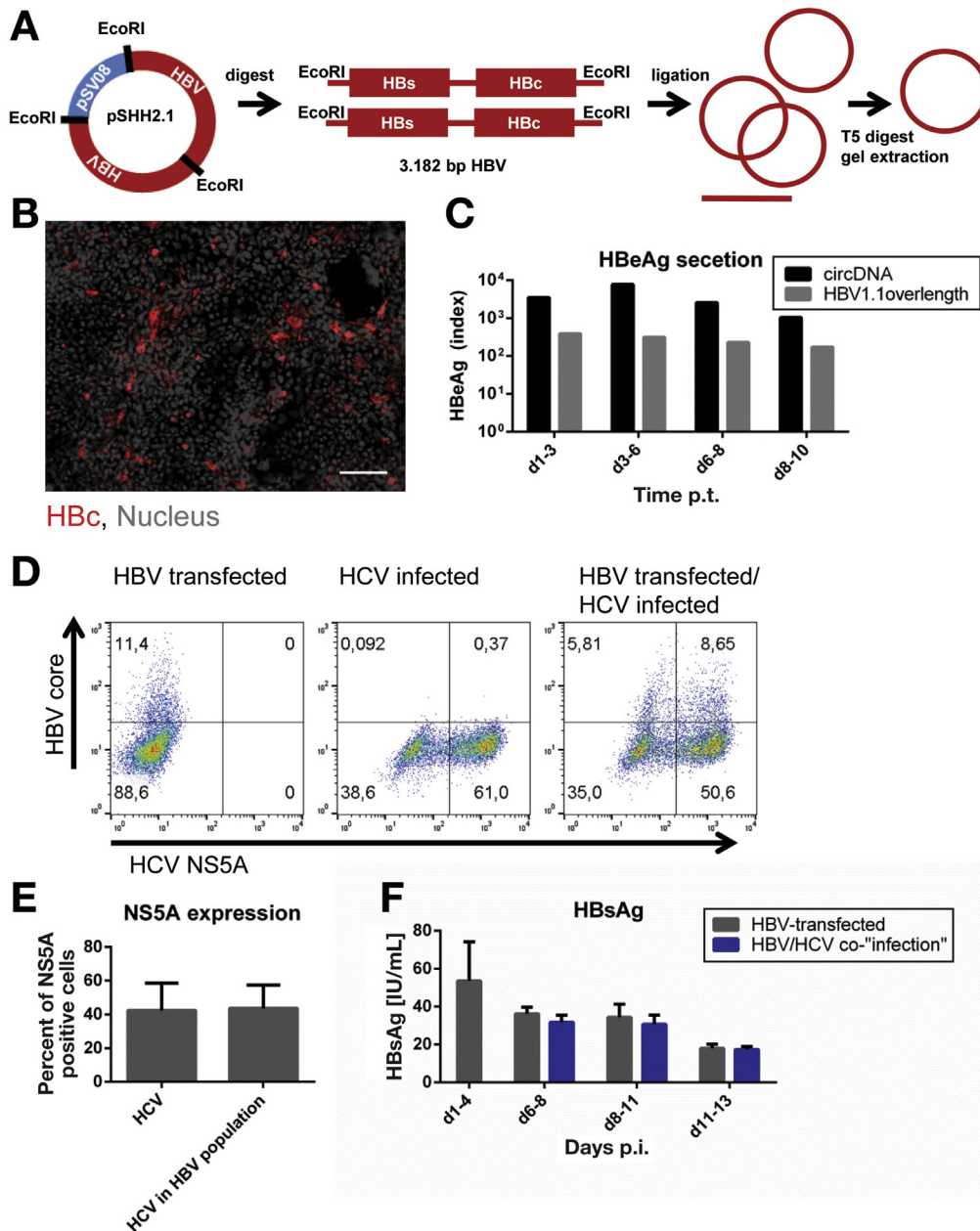


**Figure 5.** In vitro ligated, circular (circ) HBV genomes support viral replication and allow HCV superinfection in HBV-replicating cells. (A) Schematic of circHBV genome generation. HBV genomes are released from a plasmid containing 2 genome copies by EcoRI and subjected to in vitro ligation to yield circHBV genomes. Linear DNA is removed by nuclease digestion and preparative gel electrophoresis. (B) Huh7.5 cells were transfected with 200 ng circHBV and viral replication was monitored by immunofluorescence for HBV core protein (red) 7 days post transfection (p.t.). Nuclear DNA was stained with DAPI (gray). (C) Kinetics of HBeAg secretion from circHBV-transfected cells. For comparison, Huh7.5 cells were transfected with 200 ng of a 1.1 HBV overlength plasmid in which the pgRNA is transcribed under control of the cytomegalovirus promoter. (D) Huh7.5 cells were transfected with circHBV, superinfected with HCV (multiplicity of infection = 0.1) 4 days p.t. and analyzed by flow cytometry 5 days thereafter. Cells were stained for HBV core and HCV NS5A. (E) Quantification of the percentage of HCV NS5A-positive cells in HCV single infected samples (HCV) or in the HBV-positive cell population. (F) Kinetics of HBsAg secretion from either HBV transfected cells or HBV/HCV coreplicating cells.

sensors, only there does reverse transcription take place. Although these capsids are leaky to allow the passage of nucleotides, the capsid “pores” (diameter approximately 1.2–1.5 nm<sup>50</sup>) most likely are too small to allow passage of PRRs, such as RIG-I or MDA5 or cyclic GMP-AMP Synthase. Moreover, HBV DNA is transported into the nucleus inside

the nucleocapsid, thus escaping recognition during the entry process<sup>51</sup> or the assumed intracellular amplification phase via nuclear reimport of nucleocapsids.<sup>52</sup> Although being a plausible explanation, an appropriate PRR capable of sensing HBV might be lacking or too low in abundance in hepatocytes as suggested by Thomsen et al,<sup>53</sup> including

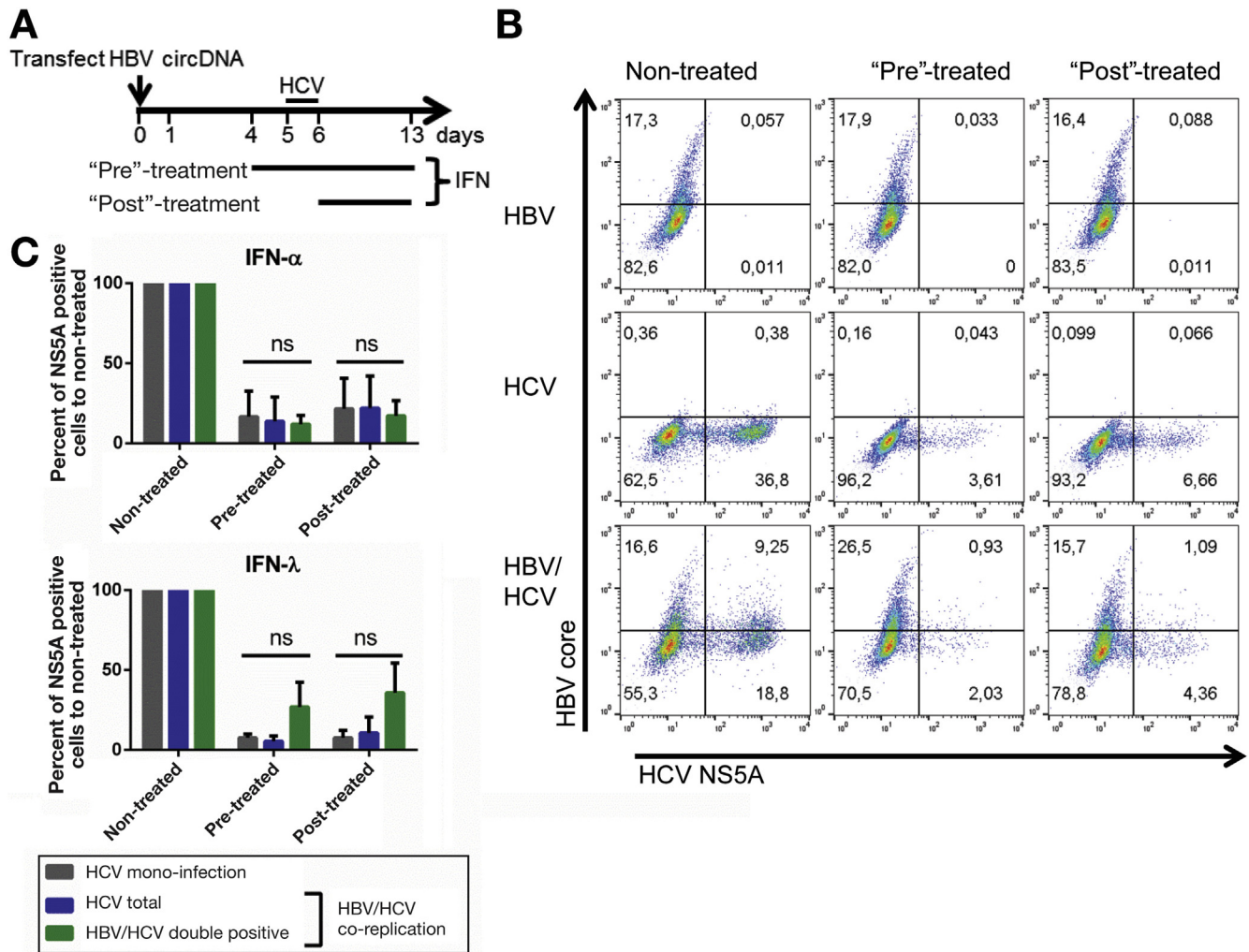


**Figure 6.** HBV does not protect HCV from the antiviral activity of IFN- $\alpha$  or IFN- $\lambda$ . (A) Schematic overview of the experimental setup. Huh7.5 cells were transfected with HBV circDNA and superinfected with HCV (multiplicity of infection = 0.1) 4 days later. Cells were treated with 100 IU/mL IFN- $\alpha$  as depicted or left untreated (control). (B) Representative experiment analyzed by flow cytometry. (C) Quantification of 3 independent experiments using either IFN- $\alpha$  (100 IU/mL) or IFN- $\lambda$  (10 ng/mL). ns, not significant.

dHepARG<sup>NTCP</sup> and PHH as used here, or expressed only in very specialized cell systems, such as micropatterned cocultures of PHH with stromal cells.<sup>18</sup> Cheng et al<sup>17</sup> could show that ectopic overexpression of the adaptor protein STING enables HepG2<sup>NTCP</sup> cells to mount an IFN response on HBV infection, supporting the hypothesis of Thomsen and colleagues.<sup>53</sup> Comparing PRR expression patterns in different cell systems should ultimately help to solve this question.

HBV is also only moderately sensitive to the antiviral state induced by IFN, as concluded from 2 observations. First, only approximately 10% of patients with CHB are able to clear the infection under pegylated IFN- $\alpha$  treatment as deduced from HBsAg seroconversion.<sup>24</sup> Second, both in infected dHepARG<sup>NTCP</sup> cells (this study) and in PHH,<sup>25</sup> treatment of HBV-infected cells with IFN had only a minor impact on viral replication. Strongest antiviral effects were observed under pretreatment conditions, consistent with a recent study suggesting that IFN triggers the release of

soluble factors blocking heparan glycosaminoglycans and inhibiting the attachment of HBV particles to cells.<sup>54</sup> Apart from such a possible entry block, our results show that IFN affects the HBV replication cycle primarily at the level of transcription or RNA translation. Considering transcription, several studies reported epigenetic silencing of cccDNA.<sup>55-57</sup> In addition, several other modes of action of IFN on HBV replication have been described, such as altering the stability of viral mRNAs,<sup>58-60</sup> blocking pgRNA packaging,<sup>41,61,62</sup> accelerating the degradation of viral nucleocapsids,<sup>63</sup> and suppression of virus particle secretion via Tetherin.<sup>64</sup> In addition, an IFN-induced cccDNA degradation via APOBEC 3A (apolipoprotein B mRNA editing enzyme catalytic subunit) has been reported.<sup>25,65</sup> Surprisingly, we observed little effect of IFN- $\alpha$  on cccDNA levels using qPCR or Southern blot, which might be due to poor up-regulation of APOBECs compared with other ISGs in our cells (Supplementary Figure 9E). APOBEC mRNA up-regulation was also low after stimulation of the IFN response with Mengo<sup>Zn</sup> in PHHs

and dHepaRG<sup>NTCP</sup> cells, arguing for weak induction of APOBECs in hepatocytes in general (Supplementary Figure 9E and F).

Several studies reported an active block of the IFN signaling cascade and subsequent ISG expression by HBV. By using uPA/SCID mice repopulated with PHH, Lütgehetmann and coworkers<sup>30</sup> detected an inhibition of nuclear translocation of STAT1 in IFN- $\alpha$  treated HBV-infected animals, which is at variance to our observation. Although the reason for this discrepancy is not clear, we note that unaltered IFN signaling as found by us is consistent with studies conducted by Chen et al<sup>66</sup> using HepG2.215 cells, and by Suslov et al, who used HBV-positive human liver biopsies (personal communication, 2017). Moreover, results obtained with the HBV/HCV coreplication model corroborate our conclusion that HBV does not block the IFN-induced antiviral state, because in individual HBV/HCV double-positive cells, HCV is efficiently suppressed by IFN, whereas HBV is not.

Although the use of the HBV/HCV coreplication system as reported here is superior to earlier systems based on the inducible expression and replication of HBV,<sup>32</sup> it still has some limitations. Notably, unambiguous detection of de novo HBV DNA replication is not possible due to high amounts of HBV circDNA required for transfection; nevertheless, infectious HBV is produced (Supplementary Figure 14). Moreover, although HBV circDNA was found to be associated with histones comparable to cccDNA,<sup>67</sup> the epigenetic modifications induced by IFN treatment might differ. In any case, the HBV/HCV coreplication system is robust and can be used to study both viruses at the single-cell level. For instance, we found that suppression of HCV with the direct-acting antivirals Sofosbuvir or Daclatasvir had no effect on HBV (Supplementary Figure 17), consistent with the assumption that HBV reactivation in treated patients appears to be immune-mediated.<sup>68</sup>

In conclusion, by using immune-competent cell culture models, we show that HBV does not induce an IFN response in hepatocytes. This absent sensing is neither due to a block of RIG-I, MDA5, or TLR3 signaling nor to an inhibition of the Jak-STAT signaling pathway and subsequent ISG activation. Collectively, our single-cell-based functional studies strengthen the notion of HBV being a “stealth” virus bypassing the IFN system.

## Supplementary Material

Note: To access the supplementary material accompanying this article, visit the online version of *Gastroenterology* at [www.gastrojournal.org](http://www.gastrojournal.org), and at <https://doi.org/10.1053/j.gastro.2018.01.044>.

## References

- World Health Organization. Global Hepatitis Report 2017. Volume Licence: CC BY-NC-SA 3.0 IGO. Available at: <http://www.who.int/hepatitis/publications/global-hepatitis-report2017/en/>; Geneva: World Health Organization, 2017:83.
- Tu T, Buhler S, Bartenschlager R. Chronic viral hepatitis and its association with liver cancer. *Biol Chem* 2017; 398:817–837.
- Caccamo G, Saffioti F, Raimondo G. Hepatitis B virus and hepatitis C virus dual infection. *World J Gastroenterol* 2014;20:14559–14567.
- Meylan E, Curran J, Hofmann K, et al. Cardif is an adaptor protein in the RIG-I antiviral pathway and is targeted by hepatitis C virus. *Nature* 2005;437: 1167–1172.
- Hiet MS, Bauhofer O, Zayas M, et al. Control of temporal activation of hepatitis C virus-induced interferon response by domain 2 of nonstructural protein 5A. *J Hepatol* 2015;63:829–837.
- Su AI, Pezacki JP, Wodicka L, et al. Genomic analysis of the host response to hepatitis C virus infection. *Proc Natl Acad Sci U S A* 2002;99:15669–15674.
- Heim MH, Thimme R. Innate and adaptive immune responses in HCV infections. *J Hepatol* 2014;61:S14–S25.
- Metz P, Reuter A, Bender S, et al. Interferon-stimulated genes and their role in controlling hepatitis C virus. *J Hepatol* 2013;59:1331–1341.
- Carreno V. Present treatment expectations and risks of chronic hepatitis C. *Clin Microbiol Infect* 2002;8:74–79.
- Nassal M. HBV cccDNA: viral persistence reservoir and key obstacle for a cure of chronic hepatitis B. *Gut* 2015; 64:1972–1984.
- Faure-Dupuy S, Lucifora J, Durantel D. Interplay between the Hepatitis B virus and innate immunity: from an understanding to the development of therapeutic concepts. *Viruses* 2017;9(5).
- Yan H, Zhong G, Xu G, et al. Sodium taurocholate cotransporting polypeptide is a functional receptor for human hepatitis B and D virus. *Elife* 2012;1:e00049.
- Wieland S, Thimme R, Purcell RH, et al. Genomic analysis of the host response to hepatitis B virus infection. *Proc Natl Acad Sci U S A* 2004;101:6669–6674.
- Stacey AR, Norris PJ, Qin L, et al. Induction of a striking systemic cytokine cascade prior to peak viremia in acute human immunodeficiency virus type 1 infection, in contrast to more modest and delayed responses in acute hepatitis B and C virus infections. *J Virol* 2009;83: 3719–3733.
- Dunn C, Peppas D, Khanna P, et al. Temporal analysis of early immune responses in patients with acute hepatitis B virus infection. *Gastroenterology* 2009;137:1289–1300.
- Niu C, Livingston CM, Li L, et al. The Smc5/6 complex restricts HBV when localized to ND10 without inducing an innate immune response and is counteracted by the HBV X protein shortly after infection. *PLoS One* 2017; 12:e0169648.
- Cheng X, Xia Y, Serti E, et al. Hepatitis B virus evades innate immunity of hepatocytes but activates cytokine production by macrophages. *Hepatology* 2017;66: 1779–1793.
- Shlomai A, Schwartz RE, Ramanan V, et al. Modeling host interactions with hepatitis B virus using primary and induced pluripotent stem cell-derived hepatocellular systems. *Proc Natl Acad Sci U S A* 2014;111: 12193–12198.

19. Giersch K, Allweiss L, Volz T, et al. Hepatitis Delta co-infection in humanized mice leads to pronounced induction of innate immune responses in comparison to HBV mono-infection. *J Hepatol* 2015; 63:346–353.
20. Jiang J, Tang H. Mechanism of inhibiting type I interferon induction by hepatitis B virus X protein. *Protein Cell* 2010;1:1106–1117.
21. Liu Y, Li J, Chen J, et al. Hepatitis B virus polymerase disrupts K63-linked ubiquitination of STING to block innate cytosolic DNA-sensing pathways. *J Virol* 2015; 89:2287–2300.
22. Luangsay S, Gruffaz M, Isorce N, et al. Early inhibition of hepatocyte innate responses by hepatitis B virus. *J Hepatol* 2015;63:1314–1322.
23. Lebosse F, Testoni B, Fresquet J, et al. Intrahepatic innate immune response pathways are downregulated in untreated chronic hepatitis B. *J Hepatol* 2017;66: 897–909.
24. Trepo C, Chan HL, Lok A. Hepatitis B virus infection. *Lancet* 2014;384:2053–2063.
25. Lucifora J, Xia Y, Reisinger F, et al. Specific and non-hepatotoxic degradation of nuclear hepatitis B virus cccDNA. *Science* 2014;343:1221–1228.
26. Seo Y, Yano Y. Short- and long-term outcome of interferon therapy for chronic hepatitis B infection. *World J Gastroenterol* 2014;20:13284–13292.
27. Shen F, Li Y, Yang W, et al. Hepatitis B virus sensitivity to interferon-alpha in hepatocytes is more associated with cellular interferon response than with viral genotype [published online ahead of print October 23, 2017]. *Hepatology* <https://doi.org/10.1002/hep.29609>.
28. Sun D, Nassal M. Stable HepG2- and Huh7-based human hepatoma cell lines for efficient regulated expression of infectious hepatitis B virus. *J Hepatol* 2006; 45:636–645.
29. Christen V, Duong F, Bernsmeier C, et al. Inhibition of alpha interferon signaling by hepatitis B virus. *J Virol* 2007;81:159–165.
30. Lütgehetmann M, Bornscheuer T, Volz T, et al. Hepatitis B virus limits response of human hepatocytes to interferon-alpha in chimeric mice. *Gastroenterology* 2011;140:2074–2083.e1–e2.
31. Liu JY, Sheng YJ, Hu HD, et al. The influence of hepatitis B virus on antiviral treatment with interferon and ribavirin in Asian patients with hepatitis C virus/hepatitis B virus coinfection: a meta-analysis. *Virol J* 2012;9:186.
32. Bellecave P, Gouttenoire J, Gajer M, et al. Hepatitis B and C virus coinfection: a novel model system reveals the absence of direct viral interference. *Hepatology* 2009; 50:46–55.
33. Ni Y, Lempp FA, Mehrle S, et al. Hepatitis B and D viruses exploit sodium taurocholate co-transporting polypeptide for species-specific entry into hepatocytes. *Gastroenterology* 2014;146:1070–1083.
34. Krieger SE, Zeisel MB, Davis C, et al. Inhibition of hepatitis C virus infection by anti-claudin-1 antibodies is mediated by neutralization of E2-CD81-claudin-1 associations. *Hepatology* 2010;51:1144–1157.
35. Sommer C, Straehle C, Köthe U, et al. ilastik: interactive learning and segmentation toolkit. *Proceedings/Eighth IEEE International Symposium on Biomedical Imaging (ISBI)*. IEEE, 2011:230–233.
36. Kato H, Takeuchi O, Sato S, et al. Differential roles of MDA5 and RIG-I helicases in the recognition of RNA viruses. *Nature* 2006;441:101–105.
37. Weber M, Gawanbacht A, Habjan M, et al. Incoming RNA virus nucleocapsids containing a 5'-triphosphorylated genome activate RIG-I and antiviral signaling. *Cell Host Microbe* 2013;13:336–346.
38. Alexopoulou L, Holt AC, Medzhitov R, et al. Recognition of double-stranded RNA and activation of NF-kappaB by Toll-like receptor 3. *Nature* 2001;413:732–738.
39. Wang N, Liang Y, Devaraj S, et al. Toll-like receptor 3 mediates establishment of an antiviral state against hepatitis C virus in hepatoma cells. *J Virol* 2009;83: 9824–9834.
40. Rajoriya N, Combet C, Zoulim F, et al. How viral genetic variants and genotypes influence disease and treatment outcome of chronic hepatitis B. Time for an individualised approach? *J Hepatol* 2017;67:1281–1297.
41. Sato S, Li K, Kameyama T, et al. The RNA sensor RIG-I dually functions as an innate sensor and direct antiviral factor for hepatitis B virus. *Immunity* 2015;42:123–132.
42. Blight KJ, McKeating JA, Rice CM. Highly permissive cell lines for subgenomic and genomic hepatitis C virus RNA replication. *J Virol* 2002;76:13001–13014.
43. Lempp FA, Mutz P, Lipps C, et al. Evidence that hepatitis B virus replication in mouse cells is limited by the lack of a host cell dependency factor. *J Hepatol* 2016;64:556–564.
44. Will H, Cattaneo R, Koch HG, et al. Cloned HBV DNA causes hepatitis in chimpanzees. *Nature* 1982;299: 740–742.
45. Sheahan T, Imanaka N, Marukian S, et al. Interferon lambda alleles predict innate antiviral immune responses and hepatitis C virus permissiveness. *Cell Host Microbe* 2014;15:190–202.
46. Chen J, Wu M, Zhang X, et al. Hepatitis B virus polymerase impairs interferon-alpha-induced STAT activation through inhibition of importin-alpha5 and protein kinase C-delta. *Hepatology* 2013;57:470–482.
47. Wu M, Xu Y, Lin S, et al. Hepatitis B virus polymerase inhibits the interferon-inducible MyD88 promoter by blocking nuclear translocation of Stat1. *J Gen Virol* 2007; 88:3260–3269.
48. Shin EC, Sung PS, Park SH. Immune responses and immunopathology in acute and chronic viral hepatitis. *Nat Rev Immunol* 2016;16:509–523.
49. Jansen L, de Niet A, Makowska Z, et al. An intrahepatic transcriptional signature of enhanced immune activity predicts response to peginterferon in chronic hepatitis B. *Liver Int* 2015;35:1824–1832.
50. Wynne SA, Crowther RA, Leslie AG. The crystal structure of the human hepatitis B virus capsid. *Mol Cell* 1999; 3:771–780.
51. Urban S, Bartschlag R, Kubitz R, et al. Strategies to inhibit entry of HBV and HDV into hepatocytes. *Gastroenterology* 2014;147:48–64.

52. Tuttleman JS, Pourcel C, Summers J. Formation of the pool of covalently closed circular viral DNA in hepadnavirus-infected cells. *Cell* 1986;47:451–460.
53. Thomsen MK, Nandakumar R, Stadler D, et al. Lack of immunological DNA sensing in hepatocytes facilitates hepatitis B virus infection. *Hepatology* 2016;64:746–759.
54. Xia Y, Cheng X, Blossey CK, et al. Secreted interferon-inducible factors restrict hepatitis B and C virus entry in vitro. *J Immunol Res* 2017;2017:4828936.
55. Tropberger P, Mercier A, Robinson M, et al. Mapping of histone modifications in episomal HBV cccDNA uncovers an unusual chromatin organization amenable to epigenetic manipulation. *Proc Natl Acad Sci U S A* 2015;112:E5715–E5724.
56. Liu F, Campagna M, Qi Y, et al. Alpha-interferon suppresses hepadnavirus transcription by altering epigenetic modification of cccDNA minichromosomes. *PLoS Pathog* 2013;9:e1003613.
57. Belloni L, Allweiss L, Guerrieri F, et al. IFN-alpha inhibits HBV transcription and replication in cell culture and in humanized mice by targeting the epigenetic regulation of the nuclear cccDNA minichromosome. *J Clin Invest* 2012;122:529–537.
58. Uprichard SL, Wieland SF, Althage A, et al. Transcriptional and posttranscriptional control of hepatitis B virus gene expression. *Proc Natl Acad Sci U S A* 2003;100:1310–1315.
59. **Mao R, Nie H, Cai D**, et al. Inhibition of hepatitis B virus replication by the host zinc finger antiviral protein. *PLoS Pathog* 2013;9:e1003494.
60. Liu Y, Nie H, Mao R, et al. Interferon-inducible ribonuclease ISG20 inhibits hepatitis B virus replication through directly binding to the epsilon stem-loop structure of viral RNA. *PLoS Pathog* 2017;13:e1006296.
61. Wieland SF, Eustaquio A, Whitten-Bauer C, et al. Interferon prevents formation of replication-competent hepatitis B virus RNA-containing nucleocapsids. *Proc Natl Acad Sci U S A* 2005;102:9913–9917.
62. **Li N, Zhang L**, Chen L, et al. MxA inhibits hepatitis B virus replication by interaction with hepatitis B core antigen. *Hepatology* 2012;56:803–811.
63. Xu C, Guo H, Pan XB, et al. Interferons accelerate decay of replication-competent nucleocapsids of hepatitis B virus. *J Virol* 2010;84:9332–9340.
64. Yan R, Zhao X, Cai D, et al. The interferon-inducible protein tetherin inhibits hepatitis B virus virion secretion. *J Virol* 2015;89:9200–9212.
65. **Xia Y, Stadler D**, Lucifora J, et al. Interferon-gamma and tumor necrosis factor-alpha produced by T cells reduce the HBV persistence form, cccDNA, without cytolysis. *Gastroenterology* 2016;150:194–205.
66. Chen H, Wang LW, Huang YQ, et al. Interferon-alpha induces high expression of APOBEC3G and STAT-1 in vitro and in vivo. *Int J Mol Sci* 2010;11:3501–3512.
67. **Yan Z, Zeng J**, Yu Y, et al. HBVcircle: a novel tool to investigate hepatitis B virus covalently closed circular DNA. *J Hepatol* 2017;66:1149–1157.
68. Konstantinou D, Deutsch M. The spectrum of HBV/HCV coinfection: epidemiology, clinical characteristics, viral interactions and management. *Ann Gastroenterol* 2015;28:221–228.

---

Author names in bold designate shared co-first authorship.

Received June 16, 2017. Accepted January 25, 2018.

#### Reprint requests

Address requests for reprints to: Ralf Bartenschlager, PhD, Department of Infectious Diseases, Molecular Virology, Heidelberg University Im Neuenheimer Feld 344, 69120 Heidelberg, Germany. e-mail: [Ralf.Bartenschlager@med.uni-heidelberg.de](mailto:Ralf.Bartenschlager@med.uni-heidelberg.de); fax: +49 6221 564570.

#### Acknowledgments

The authors are grateful to S. Bastian, U. Herian, S. Kallis, F. Schlund, J. Mohr, and S. Durant for excellent technical assistance and invaluable support and to F. Huschmand and T. Holz for technical and IT assistance. Further, the authors cordially thank Stefan Schäfer (Rostock), Jessika Sonnabend, and Yi Ni for providing the HBV genotype C2 pcDNA 1.1mer plasmid. The authors also thank R. Zawatzki (Heidelberg), G. Kochs (Freiburg), F. Weber (Gießen), Frank van Kuppeveld (Utrecht), and Charles Rice (New York) for providing materials and methods.

Philippe Metz's present address: Roche Diagnostics GmbH, Mannheim, Germany. Silke Bender's present address: Knoell Consult GmbH, Mannheim, Germany. Agnese Restuccia's present address: Gilead Sciences srl, Milano, Italy. Peter Schemmer's present address: Division of General, Visceral and Transplant Surgery, Department of Surgery, Medical University of Graz, Austria.

#### Conflicts of interest

The authors disclose no conflicts.

#### Funding

Deutsche Forschungsgemeinschaft, SFB/TRR179, TP9 to Ralf Bartenschlager; TP11 to Marco Binder; TP16 to Stephan Urban; and InfectEra HBVccc to Thomas F. Baumert.

## Supplementary Material and Methods

### Cell Lines

All cells were incubated at 37°C, 5% CO<sub>2</sub> and 95% humidity. HepaRG<sup>NTCP</sup> and HepaRG<sup>NTCP</sup> GFP-IRF3 cells were generated by lentiviral transduction as described earlier,<sup>1</sup> selected for NTCP expression by using 5 µg/mL puromycin and for GFP-IRF3 expression by using 5 µg/mL blasticidin and cultured and differentiated as described elsewhere.<sup>2</sup> Differentiated HepaRG<sup>NTCP</sup> cells were used for most of the infection experiments, as they are phenotypically closer to PHHs, including the response to IFN.<sup>3</sup> Further, as most studies were based on single selected cell clones of HepG2<sup>NTCP</sup> cells, we used dHepaRG<sup>NTCP</sup> cells to avoid clonal effects. Huh7.5 and Huh7 cells containing a stable HCV luciferase replicon<sup>4</sup> were cultured in Dulbecco's modified Eagle's medium (Life Technologies, Germany) containing 10% fetal calf serum, 1x nonessential amino acids (Life Technologies, Darmstadt, Germany), 100 µg/mL penicillin, and 100 µg/mL streptomycin. Huh7 and Huh7.5 cells were seeded at a density of 8 × 10<sup>4</sup> and 1.6 × 10<sup>5</sup> cell/mL, respectively. HepG2<sup>NTCP</sup> cells were cultured like Huh7.5 cells and used only for the experiment shown in [Supplementary Figure 14E](#). Four percent PEG was present in the inoculation medium and 2% dimethyl sulfoxide was added to the culture medium throughout the whole experimental period.

### Virus Stocks, poly(I:C), IFN, and DAAs

HBV genotype D was purified as previously described.<sup>5</sup> In brief, HBV contained in culture supernatant of HepAD38 cells was purified by heparin affinity chromatography. HBV genotype C2 was generated by transfecting a pcDNA3.1(+) HBV1.1 overlength construct into Huh7 cells. Medium was changed 24 hours post transfection. Supernatant was collected from days 3 to 5, 5 to 7, and 7 to 9, filtered through a 0.45-µm sieve, pooled, and purified by heparin affinity chromatography. HBV genome equivalents (GEs) were determined by qPCR at the virological diagnostic center of the University Hospital Heidelberg. Cells were inoculated with HBV (100 GEs/cell) in the presence of 4% polyethylene glycol (PEG) 8000 for 24 hours. After infection, cells were washed 3 times with PBS. Rift valley fever virus encoding Renilla luciferase in lieu of the NSs protein (RVFVΔNSs) (kind gift from Friedemann Weber, Gießen, Germany) was cultured in BHK cells. The virus was titrated on dHepaRG<sup>NTCP</sup> cells by inoculation with serial dilutions and measurement of luciferase activity 24 hours later. The Mengo<sup>Zn</sup> virus mutant (ie, a Mengo virus containing a mutation in the zinc binding domain of the viral leader protein<sup>6</sup>) was a kind gift of Frank van Kuppeveld (University Utrecht) and was amplified as reported.<sup>6</sup> Titers of infectious virus were determined by limiting dilution assay on BHK cells (tissue culture infection dose 50% [TCID<sub>50</sub>]) as described earlier.<sup>7</sup> Sendai virus (kindly provided by Rainer Zawatzki, Heidelberg, Germany) was amplified in LSL Valo SPF embryonic chicken eggs

(Lohmann Tierzucht, Cuxhaven, Germany) as described previously<sup>1</sup> and titrated on Hela cells. Cell-culture derived HCV JC1 (HCVcc) was generated as reported.<sup>1</sup> PEG-concentrated virus stocks were titrated on Huh7.5 cells and TCID<sub>50</sub> values were determined as previously described<sup>7</sup> and by using the algorithm available under <http://www.klinikum.uni-heidelberg.de/Downloads.126386.0.html>. For TLR3 stimulation, 10 µg/mL poly(I:C) (Sigma-Aldrich, Schnellendorf, Germany) was added to the cell culture medium. IFN-α2 (PBL Laboratories, New York, NY) as well as IFN-λ1 (PeproTech, Hamburg, Germany) were used at the indicated doses and were added freshly after each medium change. Sofosbuvir (SOF) and Daclatasvir (DCV) were used at final concentrations of 727 nM and 730 nM, respectively.

### cccDNA Quantification by qPCR

cccDNA copy numbers were analyzed as reported previously.<sup>5</sup> In brief, total DNA was isolated with the NucleoSpin Tissue Kit (Macherey-Nagel, Duren, Germany) and incubated with 5 units T5 exonuclease (New England Biolabs, Ipswich, MA) for 1 hour at 37°C, followed by enzyme inactivation for 20 minutes at 70°C. qPCR was performed using the PerfeCTa qPCR Toughmix (Quanta Biosciences, Beverly, MA), cccDNA-specific primers and probe (see [Supplementary Table 3](#)) and a 2-step program (step 1: preheating: 95°C/15 minutes; step 2: annealing: 95°C/5 seconds; step 3: polymerization: 63°C/70 seconds; repeated steps 2 and 3 for 50 cycles). The pSHH2.1 plasmid<sup>8</sup> containing a head-to-tail HBV dimer served as a template for the standard. For oligonucleotide sequences see [Supplemental Table 3](#).

### cccDNA Quantification by Southern Blot

cccDNA analysis isolation and analysis is adapted from Cai et al.<sup>9</sup> Seven 10-cm-diameter dishes were used per condition. HepaRG<sup>NTCP</sup> cells were washed twice with PBS and lysed by adding 7.5 mL of lysis buffer (10 mM Tris and 10 mM EDTA pH = 7.5) and 0.5 mL of 10% sodium dodecyl sulfate per dish. After 30 minutes of incubation at room temperature, lysates were transferred into reaction tubes, 2 mL 5 M NaCl was added, and samples incubated at 4°C overnight. Samples were centrifuged for 30 minutes at 4°C in a table-top centrifuge and supernatants were extracted twice with an equal volume of phenol and once with an equal volume of phenol/chloroform/isoamylalcohol (25:24:1). After precipitation, DNA was washed with 70% ethanol and DNA from seven 10-cm-diameter dishes was dissolved in 100 µL TE buffer (10 mM Tris HCl [pH. 7.5], 1 mM EDTA). A control sample was digested with EcoRI to linearize cccDNA and 30 µL of each sample was separated by electrophoresis into a 1.2% agarose gel. The gel was depurinated by soaking for 10 minutes in freshly prepared 0.2 M HCl, denatured in 0.5 M NaOH/1.5 M NaCl for 1 hour and neutralized for 1 hour at room temperature in 1.5 M NaCl, 1 M Tris HCl [pH7.4]. Capillary gel blotting onto nylon membrane was performed overnight in 20×SSC buffer (0.3 M sodium citrate in 3M NaCl). DNA was cross-linked by UV irradiation, blots were soaked in commercial



hybridization buffer (QuikHyb 201221-21; Agilent, Santa Clara, CA) at 60°C and incubated with a [<sup>32</sup>P]-dCTP radiolabeled HBV probe (genotype D) in the same buffer overnight. The membrane was washed 4 times each for 15 minutes in 1×SSC/0.5% sodium dodecyl sulfate bound radiolabeled probe was detected by using a phosphor imager (Typhoon FLA 7000, GE Healthcare, Little Chalfont, UK). Images were quantified using the ImageJ software package (imagej.nih.gov/ij).

### Reverse-Transcriptase qPCR

Total RNA was extracted with the NucleoSpin RNA kit (Macherey-Nagel) and after DNA digestion used for reverse transcription using the Applied Biosystems (Foster City, CA) kit (#4368814) as recommended by the manufacturer. To exclude DNA contaminants, a mock reverse transcription without reverse transcriptase was performed for every sample for pgRNA quantification. qPCR was performed with a SYBR green universal mix (#172–5124; BioRad, Hercules, CA). GAPDH (glyceraldehyde-3-phosphate dehydrogenase) served as reference. The  $\Delta\Delta$ ct-method according to Livak and Schmittgen<sup>10</sup> was used to determine relative mRNA amounts. A pcDNA HBV 1.1 plasmid served as a standard to determine pgRNA copy numbers. For oligonucleotide sequences, see [Supplementary Table 3](#).

### HBV circDNA Generation and Transfection

The plasmid pSHH2.1<sup>8</sup> containing 2 copies of the HBV genotype D (subtype ayw) genome was restricted with EcoRI and excised genomes were purified by preparative agarose gel electrophoresis. Single circular HBV genomes were generated by self-ligation after high dilution of viral DNA (1 ng/ $\mu$ L DNA) by using T4 DNA ligase. After 1 hour at room temperature, DNA was concentrated by using spin columns (Macherey-Nagel NucleoSpin Gel and PCR Clean-up). To remove linear DNA molecules, samples were digested with T5 exonuclease (New England Biolabs) for 1 hour at 37°C and separated by agarose gel electrophoresis to exclude circles containing 2 or more HBV copies. Excised single circular HBV DNA genomes (HBVcirc) were eluted by using the NucleoSpin Gel and PCR Clean-up kit (Macherey-Nagel), and the concentration of purified DNA was determined by spectrophotometry. Huh7.5 cells were transfected with HBVcirc DNA ( $\sim 7.4 \times 10^5$  copies/cell) by using the Mirus (Madison, WI) TransIT transfection reagent. To keep amounts of transfected DNA constant (500 ng DNA per well of a 24-well plate) and for mock transfection the pBlue-script K (–) vector (Agilent) lacking eukaryotic promoters was used as carrier. Medium was exchanged 24 hours post transfection.

### HBeAg and HBsAg Quantification

Viral antigens contained in culture supernatants were quantified by the analytic center of the University Hospital Heidelberg. HBeAg was analyzed by the ADVIA Centaur XPTM automated chemo luminescence system (Siemens Healthcare, Erlangen, Germany) and HBsAg was quantified as international units using an enzyme-linked

immunosorbent assay (Architect; Abbott, Chicago, IL). HBeAg samples were diluted to stay in the linear range of the assay. The calibrator (recombinant HBeAg) delivered with the assay was used to calibrate the system (Ref. 01512127, Siemens ADVIA Centaur Hepatitis B e Antigen Assay). All samples within 1 experiment were measured at the same time and with a single lot to guarantee comparability.

### Taurocholate Uptake Assay

Taurocholate (TC) uptake was measured as previously described.<sup>5</sup> In brief, differentiated HepaRG<sup>NTCP</sup> cells were treated with different doses of IFN- $\alpha$  for 24 hours and incubated for 15 minutes at 37°C with 50  $\mu$ M nonradioactive TC (Sigma-Aldrich) and 5 nM [<sup>3</sup>H]-labeled TC with a specific activity of 10 Ci/mmol (Hartmann Analytic, Braunschweig, Germany). Subsequently, cells were washed 3 times with ice cold PBS, lysed with 0.05% sodium dodecyl sulfate in PBS/0.25 M NaOH, mixed with Ultima Gold liquid scintillation solution (Perkin Elmer, Waltham, MA) and incorporated radioactivity was quantified by using a LS 6000 liquid scintillation counter (Beckmann Coulter, Brea, CA).

### PreS1 Binding Assay

Differentiated HepaRG<sup>NTCP</sup> cells were treated for 24 hours with given concentrations of IFN- $\alpha$ , trypsinized, and incubated for 10 minutes with atto-488 labeled MyrcludexB (200 nM). An excess of unlabeled MyrcludexB (500 nM) served as negative control to prevent unspecific binding. Samples were measured by flow cytometry and data were analyzed with the FlowJo software package (FlowJo, LLC, Ashland, OR).

### Interferon Bio-assay

Huh7 cells containing a stable HCV luciferase replicon<sup>4</sup> were seeded into microtiter plates (24-well format) and on the next day treated with serial dilutions of IFN- $\alpha$  or IFN- $\lambda$ . Seventy-two hours later, cells were lysed with 100  $\mu$ L lysis buffer (1% Triton X-100, 25 mM glycyl-glycin [pH 7.8], 15 mM MgSO<sub>4</sub>, 4 mM EGTA, 10% glycerol [99%]) supplemented with 1 mM 1,4-Dithiothreitol added right before use and frozen at –80°C. Firefly luciferase activity was determined by applying 400  $\mu$ L luciferase assay buffer (15 mM K<sub>3</sub>PO<sub>4</sub> [pH 7.8], 25 mM glycyl-glycin [pH 7.8], 15 mM MgSO<sub>4</sub>, 4 mM EGTA) containing 1 mM DTT, 2 mM ATP, and 1 mM D-Luciferin that were added right before use. Half maximal inhibitory concentration values were calculated by using the GraphPad Prism (v6) software package (GraphPad Software, Inc, La Jolla, CA).

### Flow Cytometry

Trypsinized cells were resuspended in 5% immunoglobulin G-free bovine serum albumin (BSA), washed once with PBS/1% BSA, and fixed for 10 minutes with 4% PFA containing 0.5% saponin. Cells were washed twice with 1% BSA and incubated with the primary antibody ([Supplementary Table 1](#)) for 45 minutes in PBS containing 1% BSA and 0.5% saponin. Cells were washed 3 times with

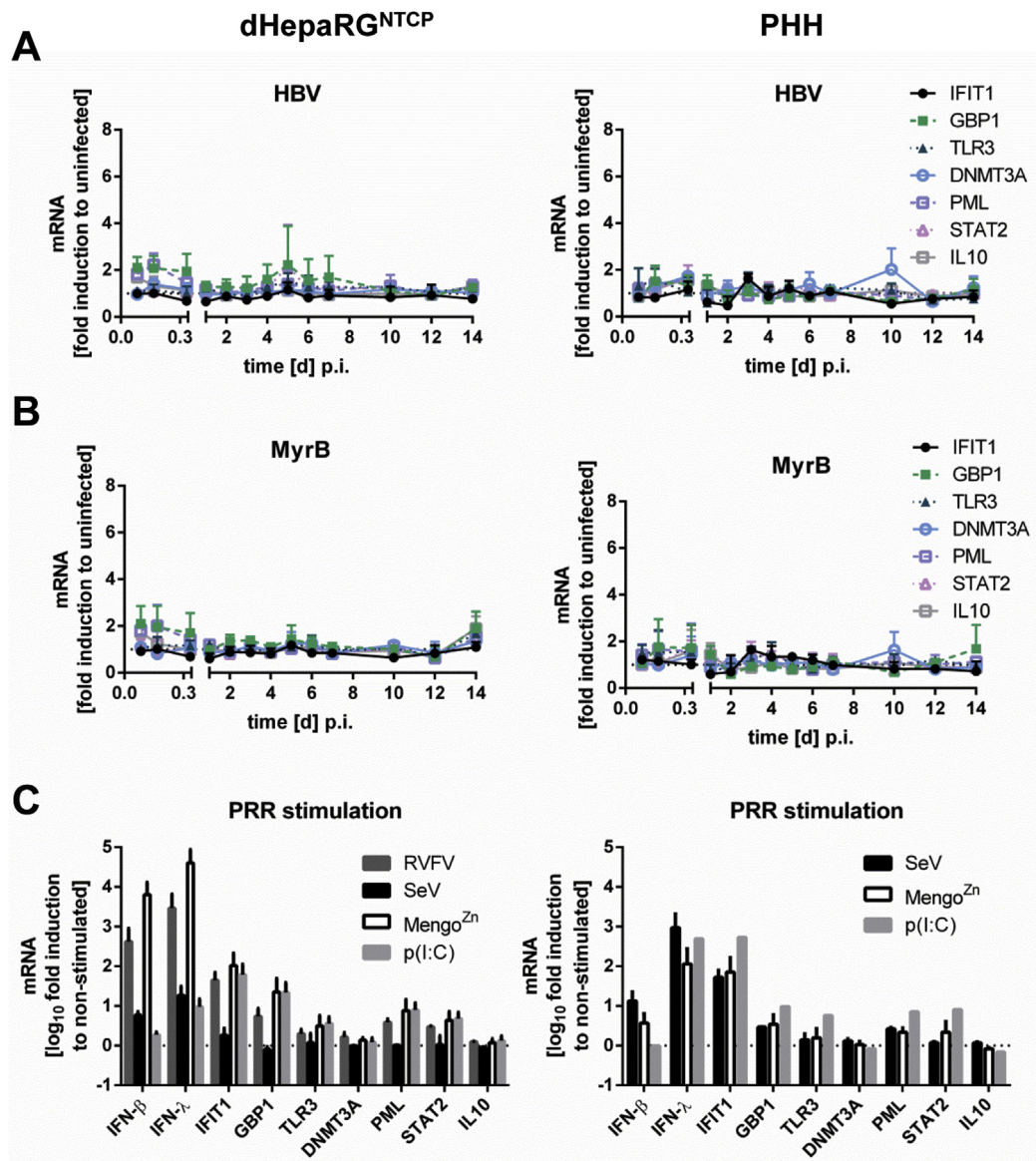
PBS, 1% BSA, and 0.5% saponin, incubated with secondary antibody (Supplementary Table 2) for 45 minutes at room temperature, and washed 3 times with PBS/1% BSA. Cells were analyzed with a BD Accuri C6 or BD Fortessa (BD Biosciences, San Jose, CA) (10,000 events per sample) and obtained data were processed with the FlowJo software package.

## References

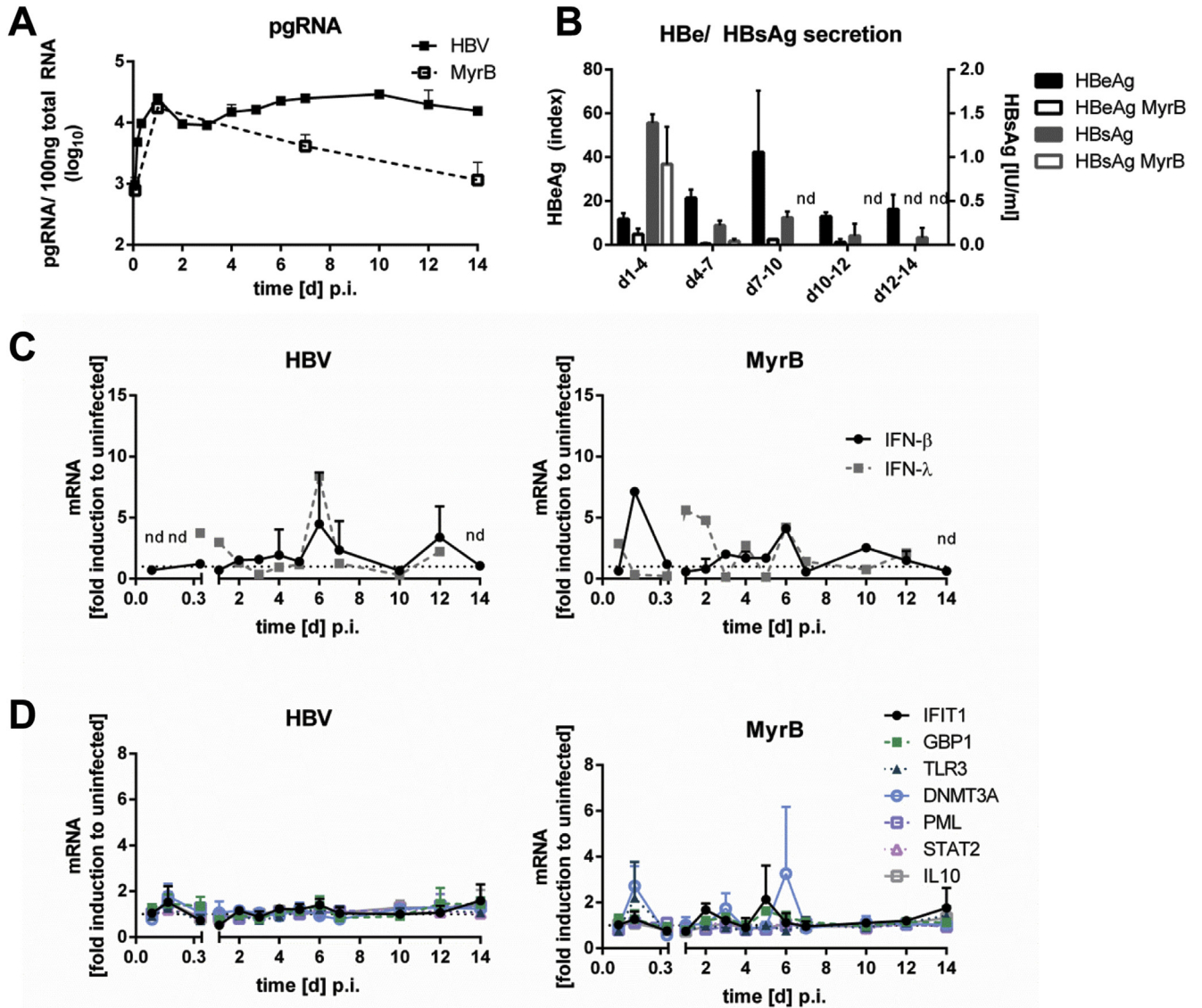
1. Bender S, Reuter A, Eberle F, et al. Activation of Type I and III interferon response by mitochondrial and peroxisomal MAVS and inhibition by Hepatitis C virus. *PLoS Pathog* 2015;11:e1005264.
2. Ni Y, Urban S. Hepatitis B virus infection of HepaRG cells, HepaRG-hNTCP cells, and primary human hepatocytes. *Methods Mol Biol* 2017;1540:15–25.
3. **Shen F, Li Y**, Yang W, et al. Hepatitis B virus sensitivity to interferon-alpha in hepatocytes is more associated with cellular interferon response than with viral genotype [published online ahead of print October 23, 2017]. *Hepatology* <https://doi.org/10.1002/hep.29609>.
4. Vrolijk JM, Kaul A, Hansen BE, et al. A replicon-based bioassay for the measurement of interferons in patients with chronic hepatitis C. *J Virol Methods* 2003;110:201–209.
5. Lempp FA, Wiedtke E, Qu B, et al. Sodium taurocholate cotransporting polypeptide is the limiting host factor of Hepatitis B Virus infection in macaque and pig hepatocytes. *Hepatology* 2017;66:703–716.
6. Hato SV, Ricour C, Schulte BM, et al. The mengovirus leader protein blocks interferon-alpha/beta gene transcription and inhibits activation of interferon regulatory factor 3. *Cell Microbiol* 2007;9:2921–2930.
7. Lindenbach BD, Evans MJ, Syder AJ, et al. Complete replication of hepatitis C virus in cell culture. *Science* 2005;309:623–626.
8. Will H, Cattaneo R, Koch HG, et al. Cloned HBV DNA causes hepatitis in chimpanzees. *Nature* 1982;299:740–742.
9. Cai D, Nie H, Yan R, et al. A southern blot assay for detection of hepatitis B virus covalently closed circular DNA from cell cultures. *Methods Mol Biol* 2013;1030:151–161.
10. Livak KJ, Schmittgen TD. Analysis of relative gene expression data using real-time quantitative PCR and the 2(-Delta Delta C(T)) Method. *Methods* 2001;25:402–408.

---

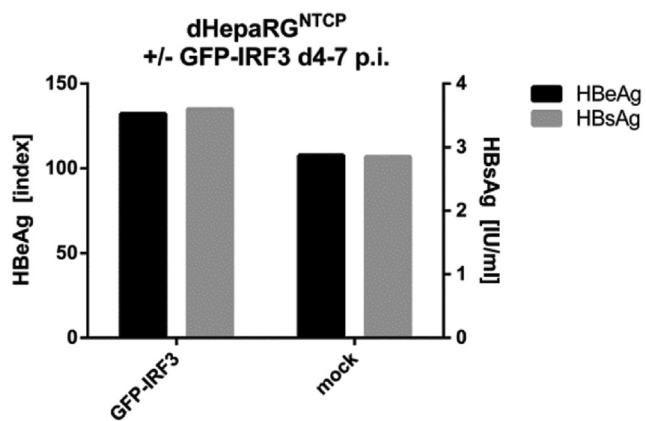
Author names in bold designate shared co-first authorship.



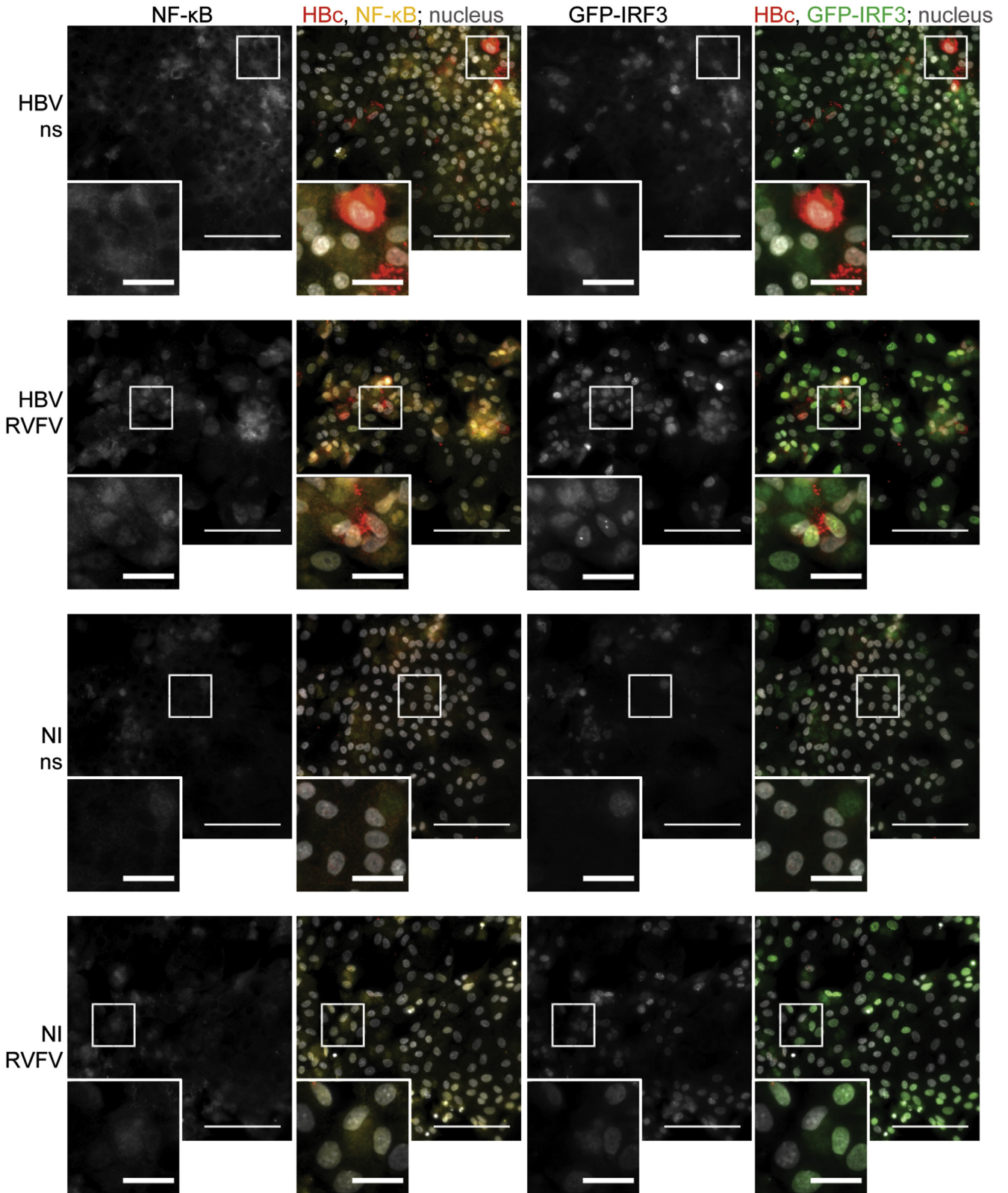
**Supplementary Figure 1.** Interferon competence of dHepaRG<sup>NTCP</sup> and PHH and lack of activation of the interferon response by HBV genotype D. (A and B) dHepaRG<sup>NTCP</sup> cells and PHHs were infected with HBV genotype D as described in the Methods section. IFIT1, GBP1, TLR3, DNMT3A, PML, STAT1, and IL10 mRNA abundance was quantified at indicated time points and normalized to the uninfected control. (C) IFN-β, IFN-λ, IFIT1, GBP1, TLR3, DNMT3A, PML, STAT1, and IL10 mRNA abundance in dHepaRG<sup>NTCP</sup> and PHH was analyzed 8 hours after infection with Sendai Virus (SeV; multiplicity of infection [MOI] = 2), or the Mengo<sup>Zn</sup> virus (Mengo<sup>Zn</sup>; MOI = 10) or after addition of 10 μg/mL p(I:C) into the cell culture supernatant. dHepaRG<sup>NTCP</sup> were additionally infected with RSVΔNSs (20x EC<sub>50</sub>) for 8 hours. Values are means and SDs from 2 independent experiments, except for p(I:C) treatment, which was once performed with PHH (only 1 donor available).



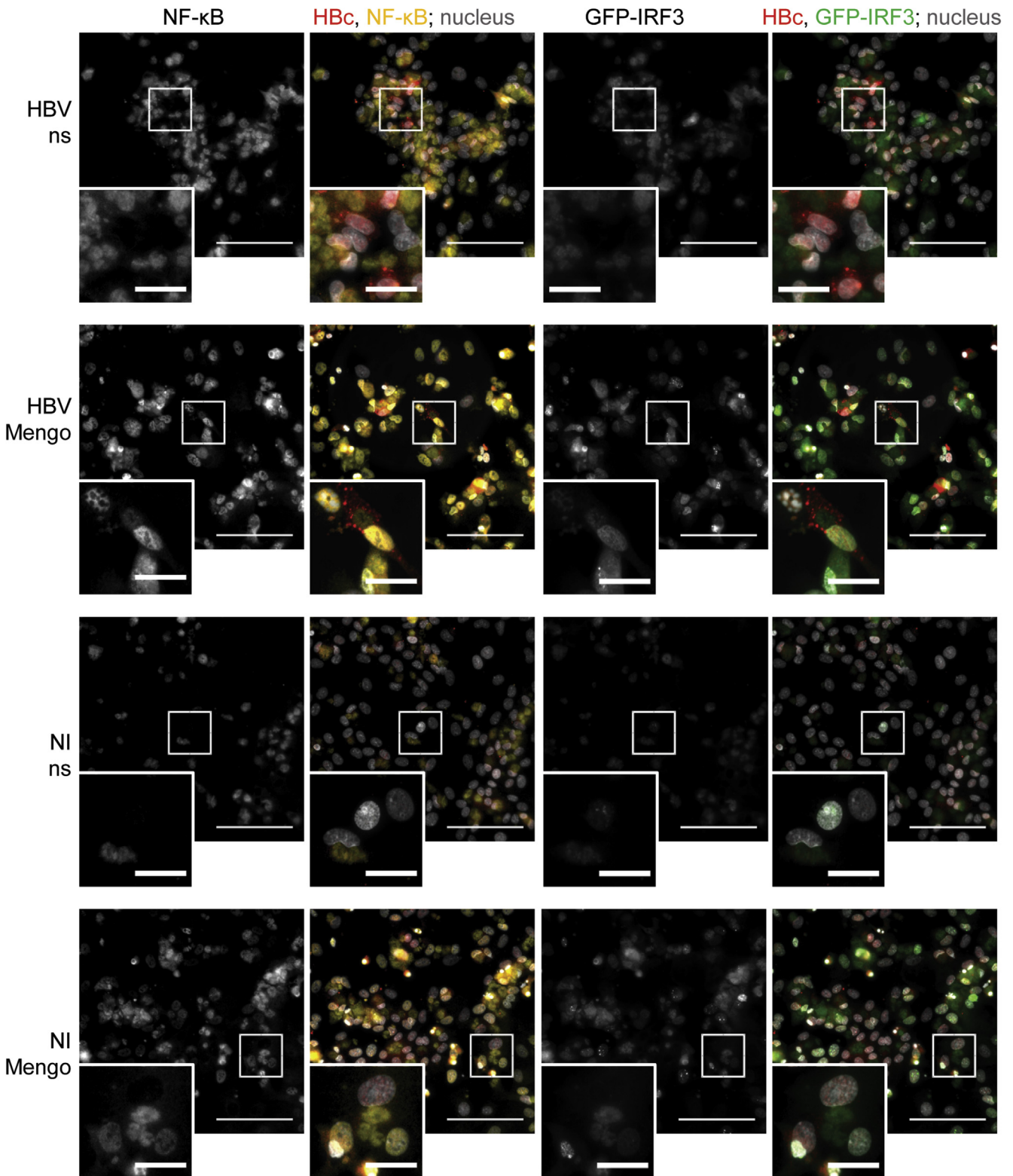
**Supplementary Figure 2.** HBV genotype C2 does not induce an interferon response in dHepaRG<sup>NTCP</sup> cells. dHepaRG<sup>NTCP</sup> cells were infected with HBV genotype C2 (100 GE/cell). (A) Time course of pgRNA accumulation in HBV-infected cells. (B) Kinetics of HBeAg and HBsAg secretion. Abundance of mRNAs of (C) IFN-β and IFN-λ1 and (D) IFIT1, GBP1, TLR3, DNMT3A, PML, STAT1, and IL10 mRNA abundance was determined by reverse-transcriptase qPCR at the indicated time points. Early time points are 2, 4, and 8 hours p.i. nd, not detectable.



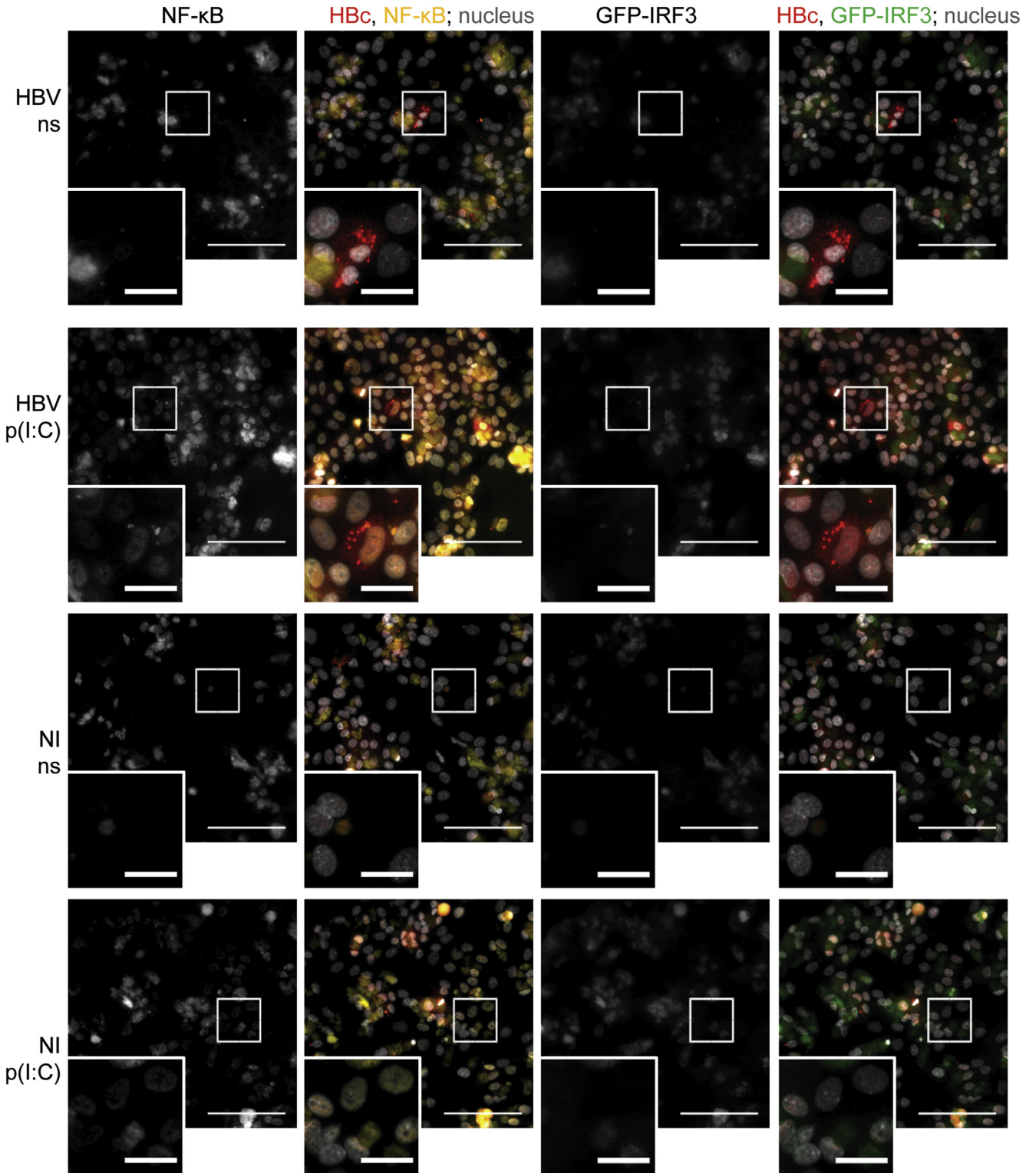
**Supplementary Figure 3.** GFP-IRF3 overexpression does not impair HBV replication. dHepaRG<sup>NTCP</sup> cells expressing either GFP-IRF3 or an empty control vector were infected with HBV for 7 days. HBeAg and HBsAg amounts accumulating in the culture supernatant between 4 and 7 days after infection are displayed. A representative experiment is shown.



**Supplementary Figure 4.** HBV does not inhibit RIG-I-mediated signaling in dHepaRG<sup>NTCP</sup> cells. (A) dHepaRG<sup>NTCP</sup> GFP-IRF3 cells were infected with HBV for 7 days and then superinfected with RVFVΔNSs (RIG-I inducer; 20x EC<sub>50</sub>) for 16 hours. Left merge shows HBV core (red), endogenous NF-κB (yellow), and nuclei (DAPI; gray). Right merge shows GFP-IRF3 (green), HBV core (red) and nuclei (DAPI; gray). Pictures were taken with a ×40 objective. Scale bar = 100 μm in the overview image and 25 μm in the zoomed insert (position indicated in the overview by white square). NI, HBV noninfected; ns, nonstimulated.

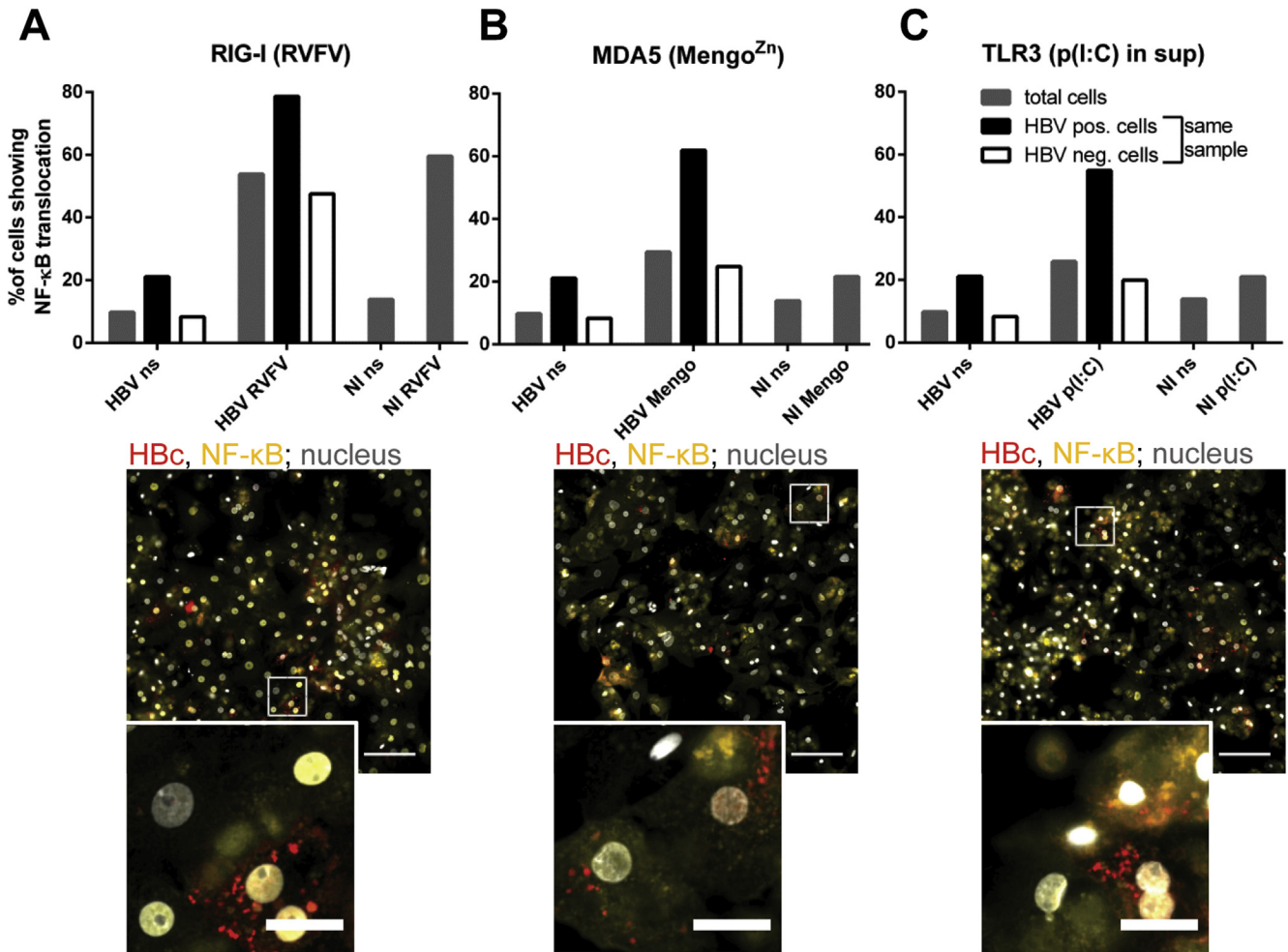


**Supplementary Figure 5.** HBV does not inhibit MDA5-mediated signaling in dHepaRG<sup>NTCP</sup> cells. (A) dHepaRG<sup>NTCP</sup> GFP-IRF3 cells were infected with HBV for 8 days and then superinfected with the Mengo<sup>Zn</sup> virus (MDA5 inducer; multiplicity of infection = 10) for 8 hours. Left merge shows HBV core (red), endogenous NF-κB (yellow), and nuclei (DAPI; gray). Right merge shows GFP-IRF3 (green), HBV core (red), and nuclei (DAPI; gray). Pictures were taken with a  $\times 40$  objective. Scale bar = 100  $\mu\text{m}$  in the overview image and 25  $\mu\text{m}$  in the zoomed insert (position indicated in the overview by white square). NI, HBV noninfected; ns, nonstimulated.

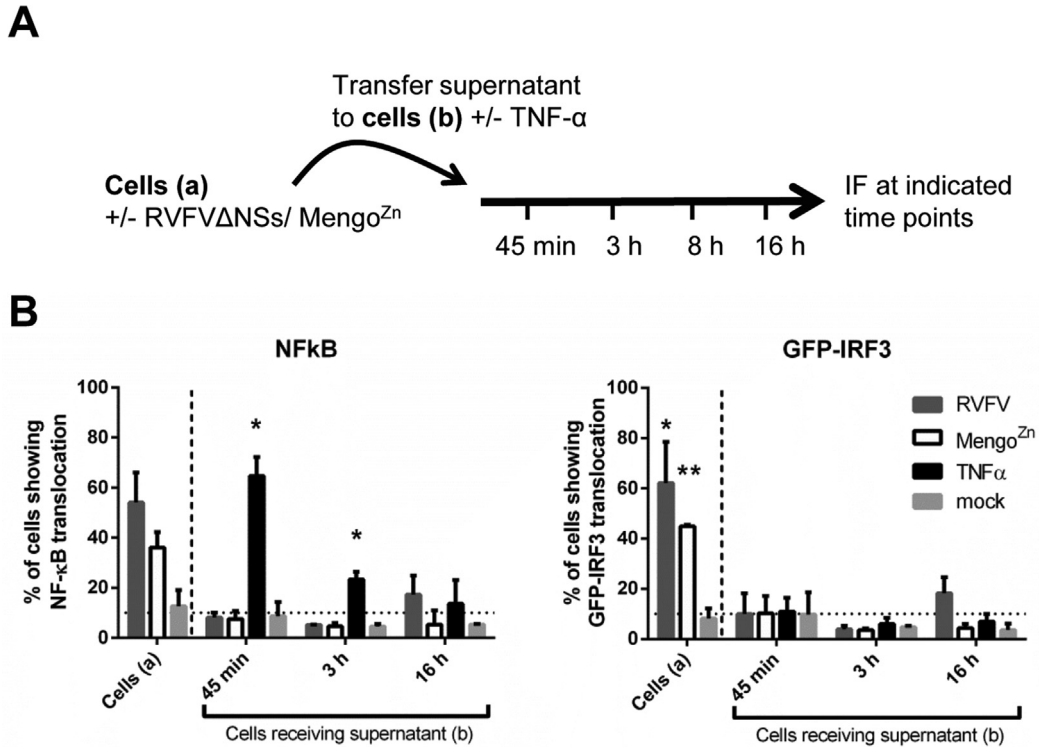


**Supplementary Figure 6.** HBV does not inhibit TLR3-mediated signaling in dHepaRG<sup>NTCP</sup> cells. (A) dHepaRG<sup>NTCP</sup> GFP-IRF3 cells were infected with HBV for 8 days and then treated with 10 μg/mL p(I:C) that was added into the culture supernatant (TLR3 inducer) for 60 minutes. Left merge shows HBV core (red), endogenous NF-κB (yellow), and nuclei (DAPI; gray). Right merge shows GFP-IRF3 (green), HBV core (red), and nuclei (DAPI; gray). Pictures were taken with a ×40 objective. Scale bar = 100 μm in the overview image and 25 μm in the zoomed insert (position indicated in the overview by white square). NI, HBV noninfected; ns, nonstimulated.

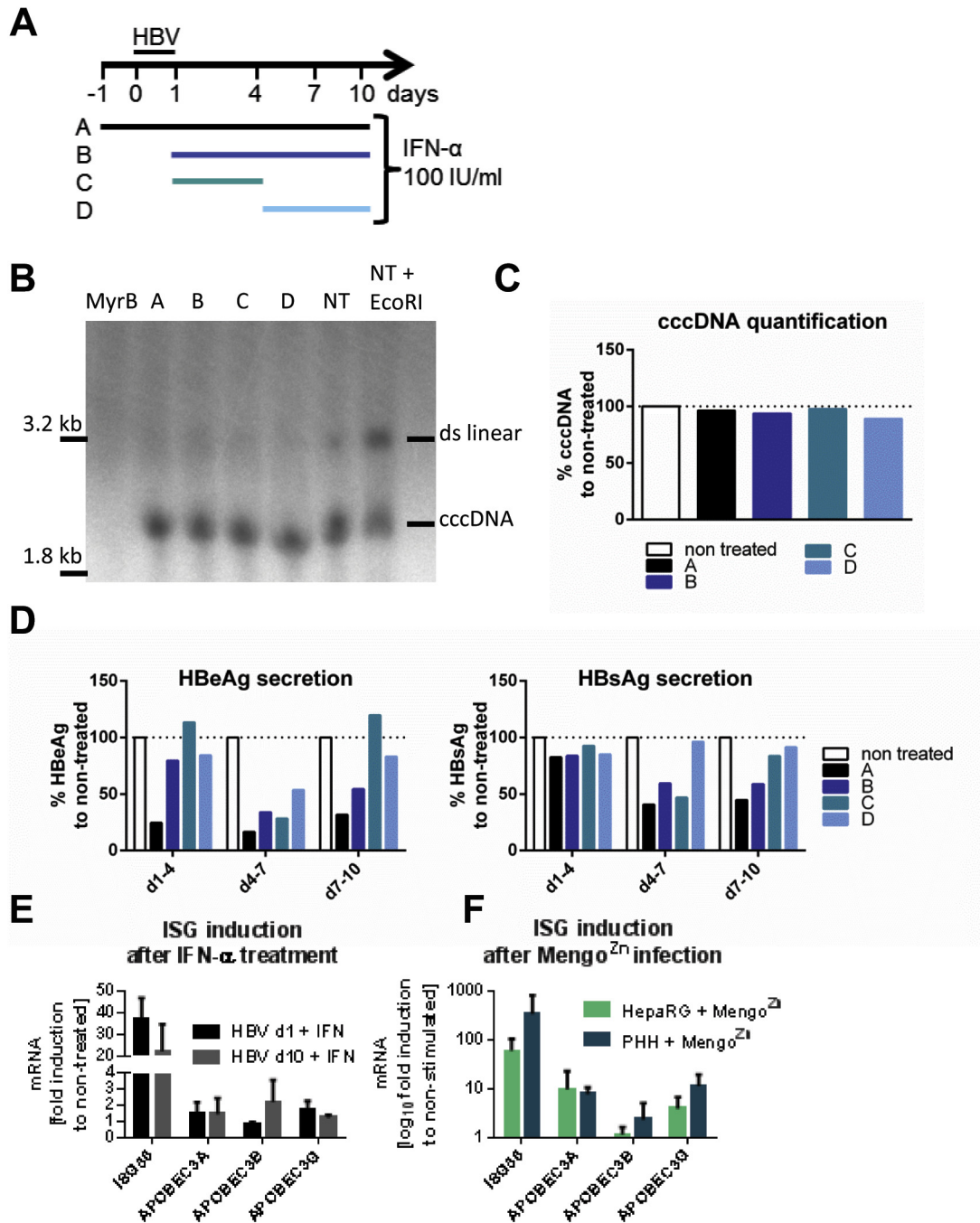




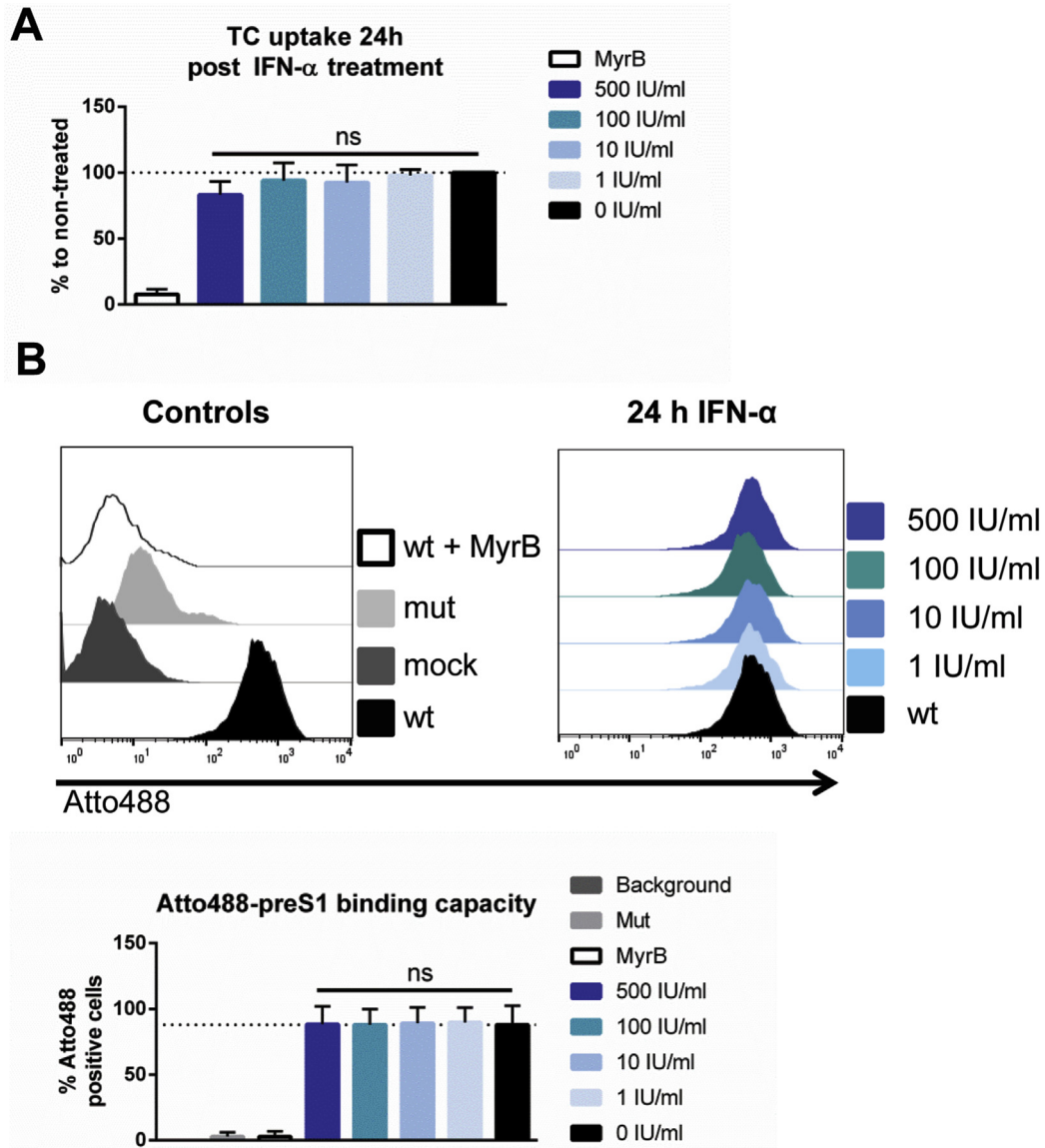
**Supplementary Figure 7.** HBV does not inhibit RIG-I, MDA5, and TLR3-mediated signaling in PHH. HBV-infected PHH were stimulated (A) at 6 days p.i. with RVFVΔNSs (RIG-I inducer; 20x EC<sub>50</sub>) for 16 hours; (B) at 7 days p.i. with the Mengo<sup>Zn</sup> virus (MDA5 inducer; multiplicity of infection = 10) for 8 hours; (C) at 7 days p.i. with 10 μg/mL poly (I:C) added into the culture supernatant for 1 hour to stimulate the TLR3 pathway. Image quantification of NF-κB translocation events in HBV-infected or noninfected (NI) cells that were stimulated or not (ns) was performed with the ILASTIK software package. Representative images are shown below each corresponding bar graph. Images were acquired with a ×10 objective. Scale bar = 200 μm in the overview image and 25 μm in the zoomed insert (position indicated in the overview by white square). HBV core (red), NF-κB (yellow), and nuclei (DAPI; gray) are shown.



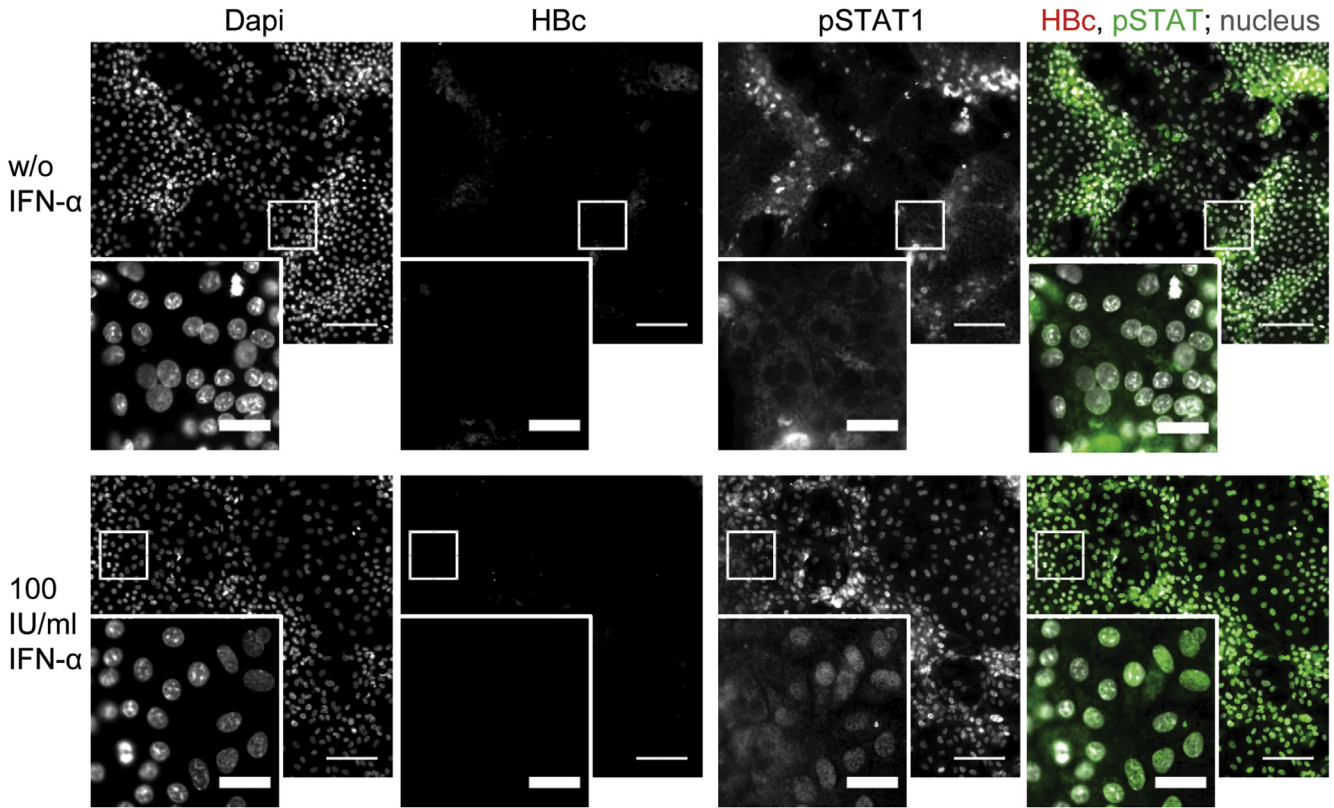
**Supplementary Figure 8.** RVFV $\Delta$ NSs or Mengo<sup>Zn</sup> virus do not induce cytokines triggering nuclear translocation of NF- $\kappa$ B or IRF3. (A) dHepaRG<sup>NTCP GFP-IRF3</sup> cells were inoculated with RVFV $\Delta$ NSs or the Mengo<sup>Zn</sup> virus and 1 hour later medium was changed, and cells incubated for another 15 and 7 hours, respectively. Supernatant was collected and transferred onto naïve dHepaRG<sup>NTCP GFP-IRF3</sup> cells which were analyzed for NF- $\kappa$ B and GFP-IRF3 translocation 45 minutes, 3 and 16 hours later by immunofluorescence. Treatment with 1 ng/mL tumor necrosis factor alpha (TNF- $\alpha$ ) served as positive control for NF- $\kappa$ B translocation. (B) Quantification of NF- $\kappa$ B and GFP-IRF3 translocation events in the infected cell (cells [a]) and cells treated with the culture supernatant (b) with or without TNF- $\alpha$ . Graph shows mean and SD from 2 independent experiments. ns, not significant; \* $P < .05$ ; \*\* $P < .01$ .



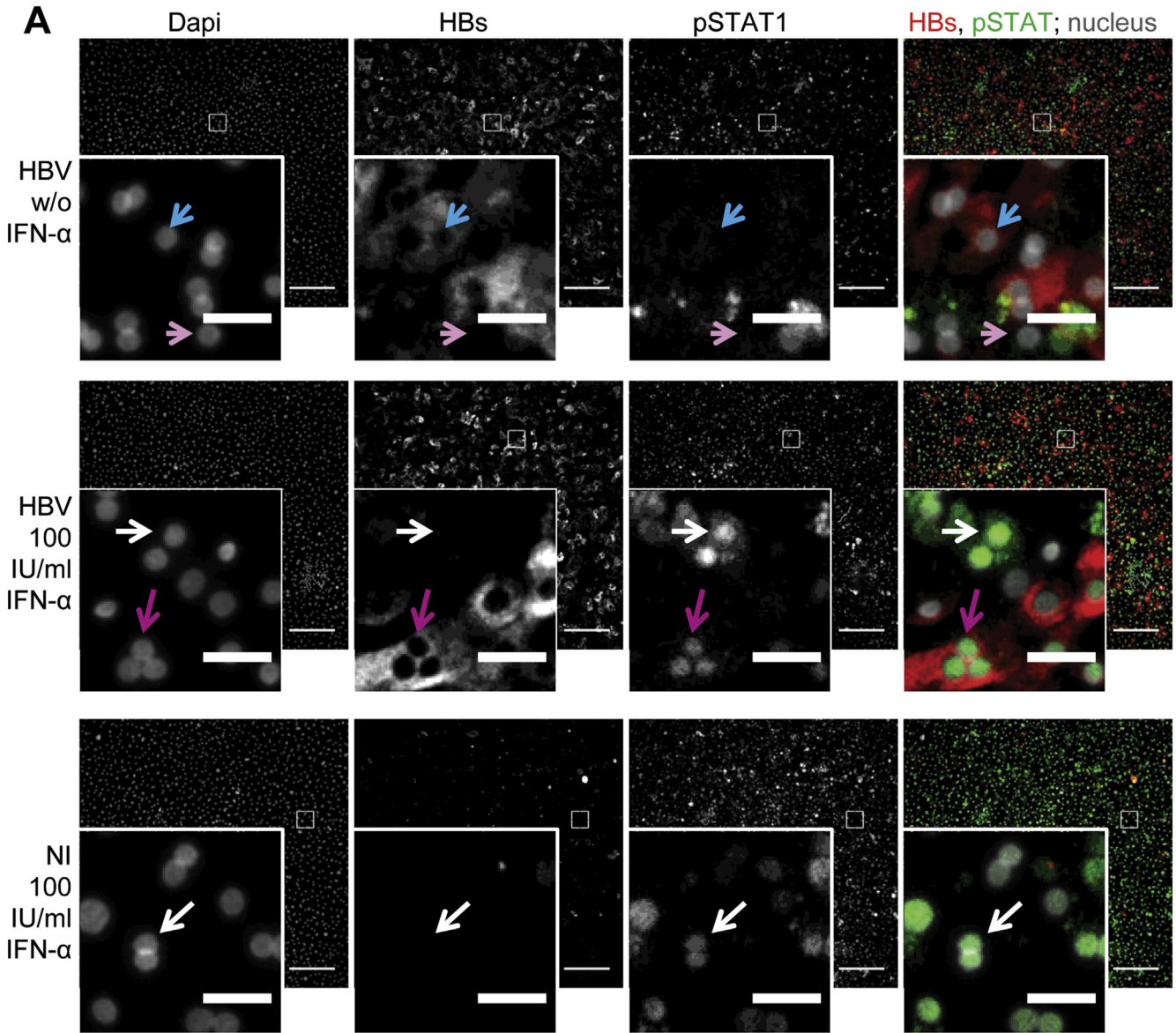
**Supplementary Figure 9.** No reduction of cccDNA by IFN- $\alpha$  treatment as determined by Southern blot. dHepaRG<sup>NTCP</sup> cells were infected with HBV (100 GE/cell) and treated with IFN- $\alpha$  as depicted in (A) and Figure 3A. After 10 days, cccDNA levels were analyzed by Southern blot and phosphor imaging (B). (C) Quantification of the phosphor imaging scan. (D) HBeAg and HBsAg levels in culture supernatants of cells that were analyzed by Southern blot (B). (E) ISG56, APOBEC 3A, 3B, and 3G mRNA levels in HBV-infected dHepaRG<sup>NTCP</sup> cells treated with IFN according to condition “A,” at day 1 and day 10 after HBV infection. Values were normalized to those obtained with HBV-infected, but nontreated cells. (F) ISG56, APOBEC 3A, 3B, and 3G mRNA levels in dHepaRG<sup>NTCP</sup> cells and PHH after infection with Mengo<sup>Zn</sup> for 8 hours. Values were normalized to mRNA levels in noninfected cells.



**Supplementary Figure 10.** IFN- $\alpha$  does not inhibit preS1 binding to NTCP. (A) dHepaRG<sup>NTCP</sup> cells were treated for 24 hours with given concentrations of IFN- $\alpha$  and analyzed for taurocholate (TC) uptake capacity by measuring the uptake of [<sup>3</sup>H]-labeled TC into the cells. n = 3. (B) dHepaRG<sup>NTCP</sup> cells were treated for 24 hours with given concentrations of IFN- $\alpha$ . After detachment of the cells, atto488-labeled Myrcludex B (corresponding to the 49 N-terminal amino acids of the HBV preS1 domain) was added, and binding capacity determined by flow cytometry. The upper panels show histograms of a representative experiment, the lower panels the quantification of 2 independent experiments. wt, wild-type atto488-MyrB mut, mutated atto488-MyrB not binding to NTCP; MyrB, unlabeled Myrcludex B, which was added in excess (500 nM) to block atto488-MyrB binding. Student *t* test was applied. ns, not significant.

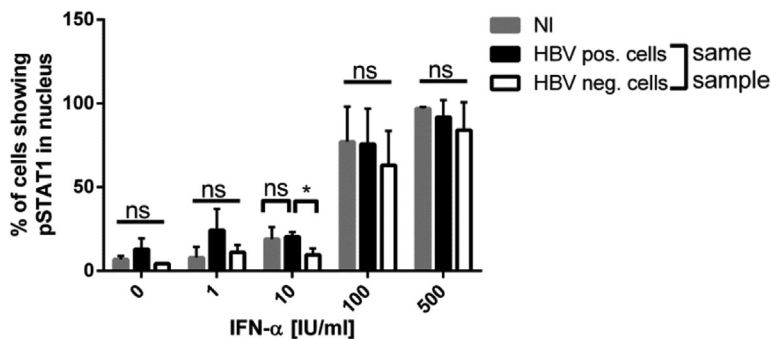


**Supplementary Figure 11.** IFN- $\alpha$  induced nuclear translocation of pSTAT1 in naïve dHepaRG<sup>NTCP</sup> cells and specificity control of HBV core protein staining. Mock-treated dHepaRG<sup>NTCP</sup> cells were incubated with either 0 or 100 IU/mL IFN- $\alpha$  for 90 minutes at 8 days post mock inoculation. Merge shows nuclei (DAPI; gray), HBV core (red), and pSTAT1 (green). Images were acquired with a  $\times 20$  objective. Scale bar = 100  $\mu$ m in overview images and 25  $\mu$ m in zoomed inserts that are indicated with white squares in the overview image. Note that shown images are also specificity controls for core protein staining shown in [Figure 4A](#).

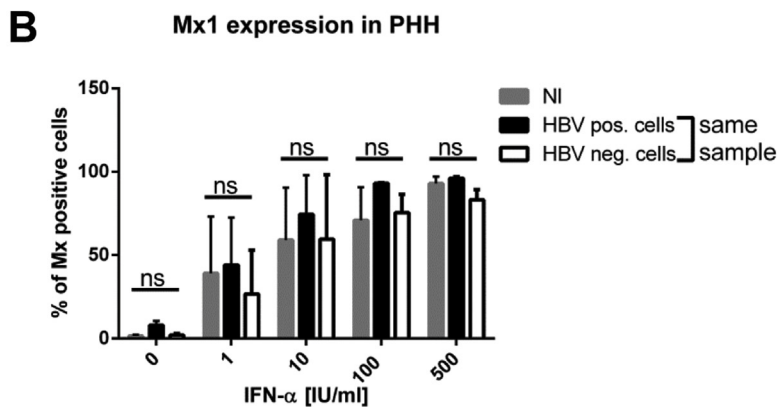
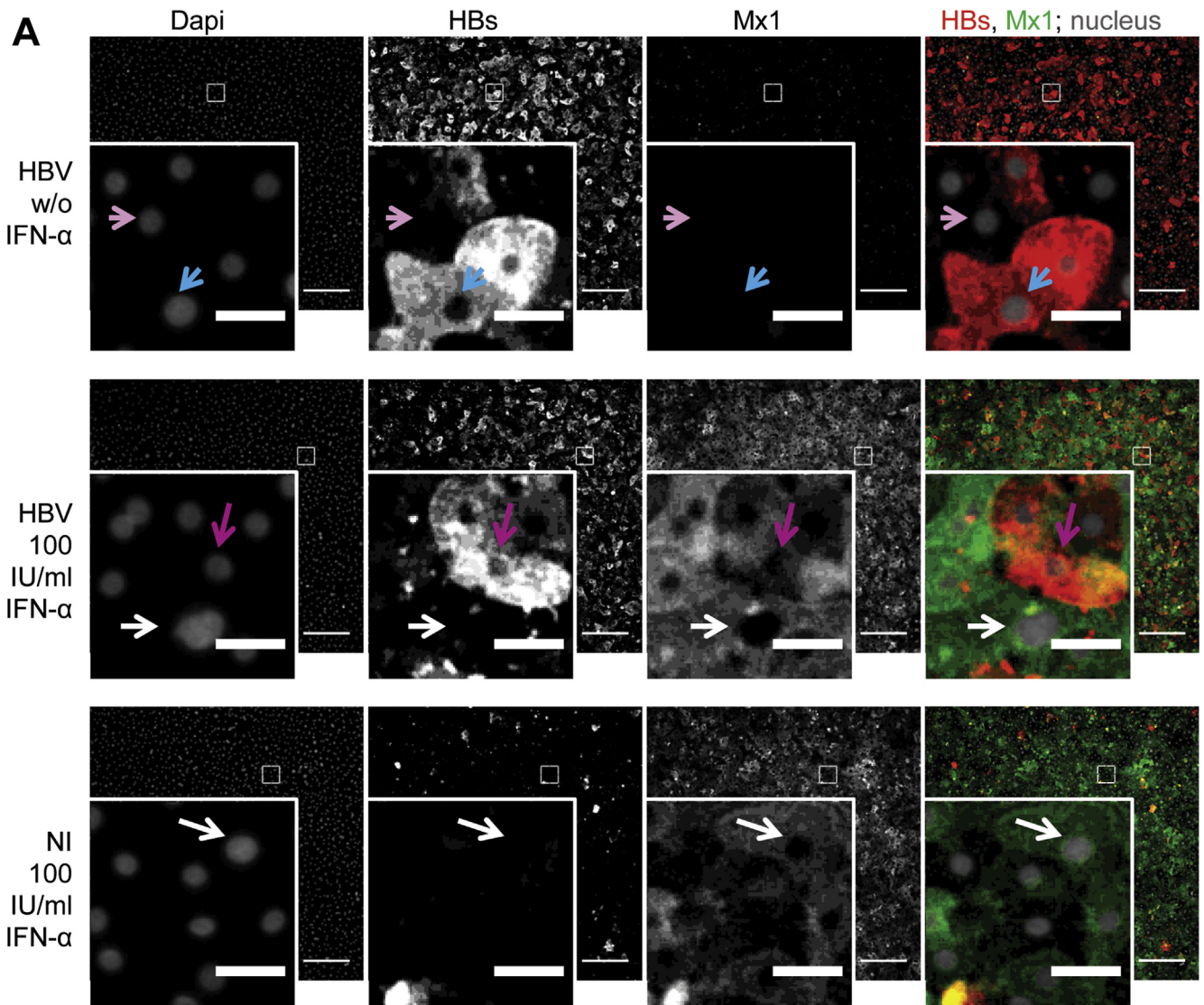


**B**

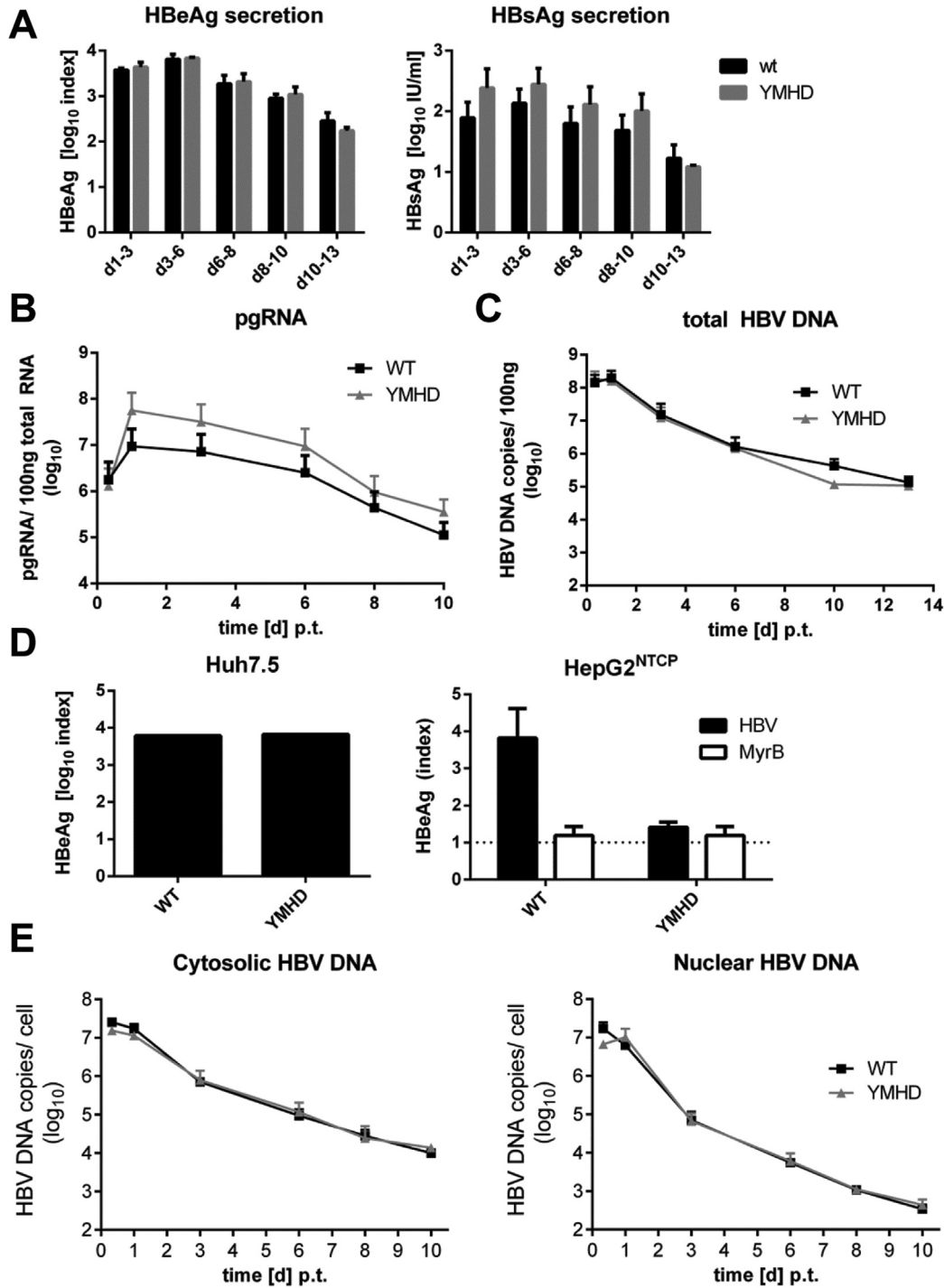
pSTAT1 translocation in PHHs



**Supplementary Figure 12.** HBV does not inhibit IFN- $\alpha$  mediated pSTAT1 translocation in PHH. HBV-infected PHH treated with given concentrations of IFN- $\alpha$  for 90 minutes at 7 days post infection were harvested for pSTAT1 analysis. (A) Representative immunofluorescence images of HBV-infected and noninfected (NI) cells treated with either 0 or 100 IU/mL IFN- $\alpha$ . Merge images show nuclear DNA (DAPI; gray), HBsAg (red), and pSTAT1 (green). Light blue arrows indicate HBV-infected cells without pSTAT1 translocation; rosy arrows mark noninfected cells without translocation; pink arrows highlight HBV-infected cells with pSTAT1 translocation; white arrows point to noninfected cells with nuclear pSTAT1. Images were acquired with a  $\times 10$  objective. Scale bars = 200  $\mu\text{m}$  in the overview image and 25  $\mu\text{m}$  in the zoomed insert (indicated with white square in the overview). (B) Quantification of 3 independent experiments as shown in (A).



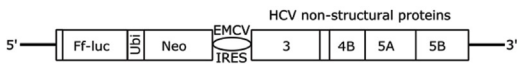
**Supplementary Figure 13.** HBV does not inhibit IFN- $\alpha$  induced Mx1 activation in PHH. HBV-infected PHH treated with given concentrations of IFN- $\alpha$  for 24 hours at 6 days p.i. were harvested for Mx1 analysis. (A) Representative immunofluorescence images of HBV-infected and noninfected (NI) cells treated with either 0 or 100 IU/mL IFN- $\alpha$ . Merge images show nuclear DNA (DAPI; gray), HBsAg (red), and pSTAT1 (green). Light blue arrows indicate HBV-infected cells without Mx1 expression; rosy arrows mark noninfected cells without Mx1; pink arrows highlight HBV-infected cells expressing Mx1; white arrows point to noninfected cells with Mx1. Images were acquired with a  $\times 10$  objective. Scale bars = 200  $\mu\text{m}$  in the overview image and 25  $\mu\text{m}$  in the zoomed insert (indicated with white square in the overview). (B) Quantification of 2 independent experiments as shown in (A).



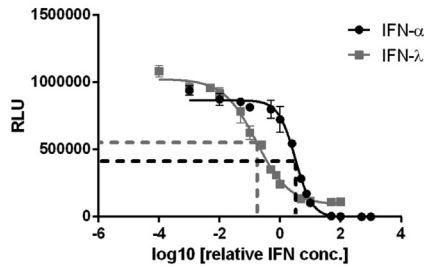
**Supplementary Figure 14.** HBV circDNA serves as a template for HBV replication. Huh7.5 cells were transfected with wild-type (wt) HBV circDNA or a reverse-transcriptase dead mutant (YMHD). The following time-course analyses were performed: (A) HBeAg and HBsAg secreted to the culture supernatant; (B) pgRNA abundance in transfected cells as determined by reverse-transcriptase qPCR; and (C) total HBV DNA in transfected cells as determined by qPCR. (D) Supernatant (days 2–9) from Huh7.5 cells transfected with wt circDNA (WT) or YMHD mutant circDNA (YMHD) was directly used to infect HepG2<sup>NTCP</sup> cells. Entry inhibitor MyrB (200 nM) added during inoculation served as infection control. HBeAg accumulating in the culture supernatant of infected HepG2<sup>NTCP</sup> cells between days 4 and 7 p.i. was quantified by using a chemo luminescence system. (E) Cytoplasm and nucleus were separated by differential centrifugation and HBV DNA contained in these fractions was quantified by qPCR. An HBV encoding plasmid was used as standard to calculate absolute numbers. Copy numbers per cell were estimated by assuming 6.6 pg DNA/cell. n = 2. Note that the HBV mutant was used to monitor the decay of HBV circDNA that was comparable between wild-type and this mutant. Owing to the high amount of transfected circDNA, de novo synthesis of HBV DNA cannot be quantified during the 10-days observation period, but infectious virus is produced (E). Importantly, this system does not rely on the expression of single viral proteins and is devoid of heterologous sequences, and therefore well suited to monitor IFN sensitivity of HBV.



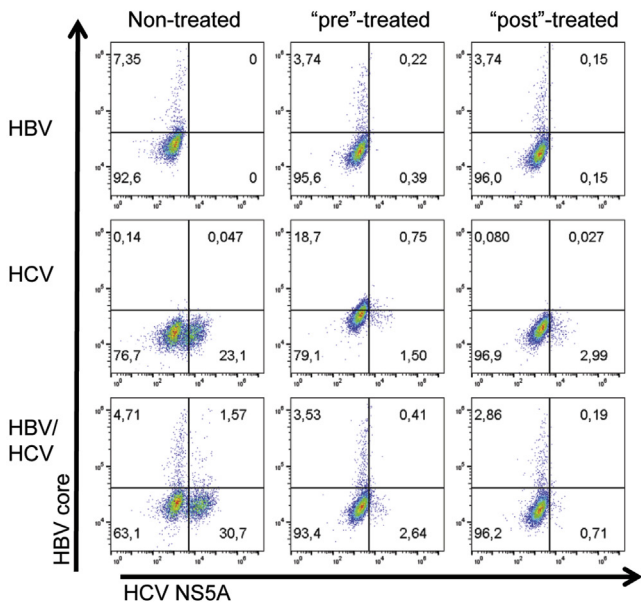
**A**



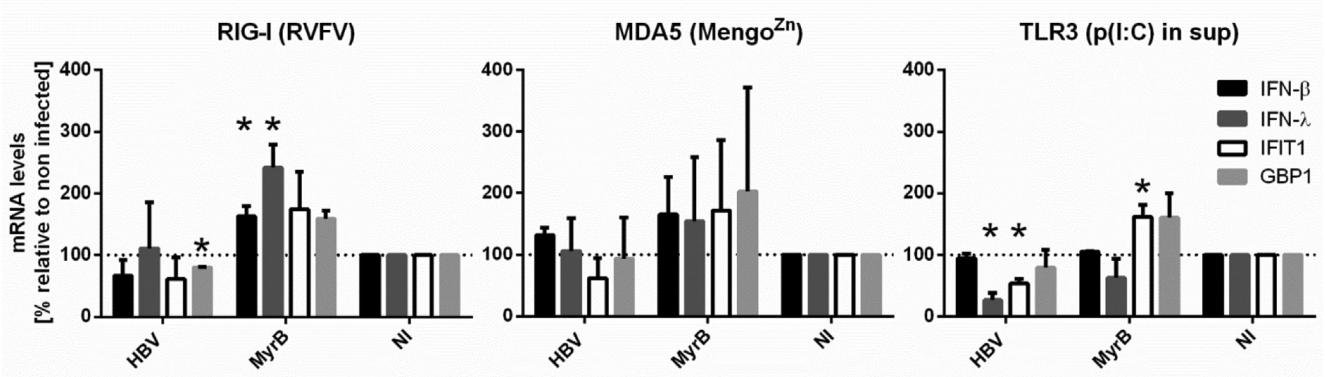
**IFN titration on Huh7  
HCV<sub>luc</sub> replicon cell line**



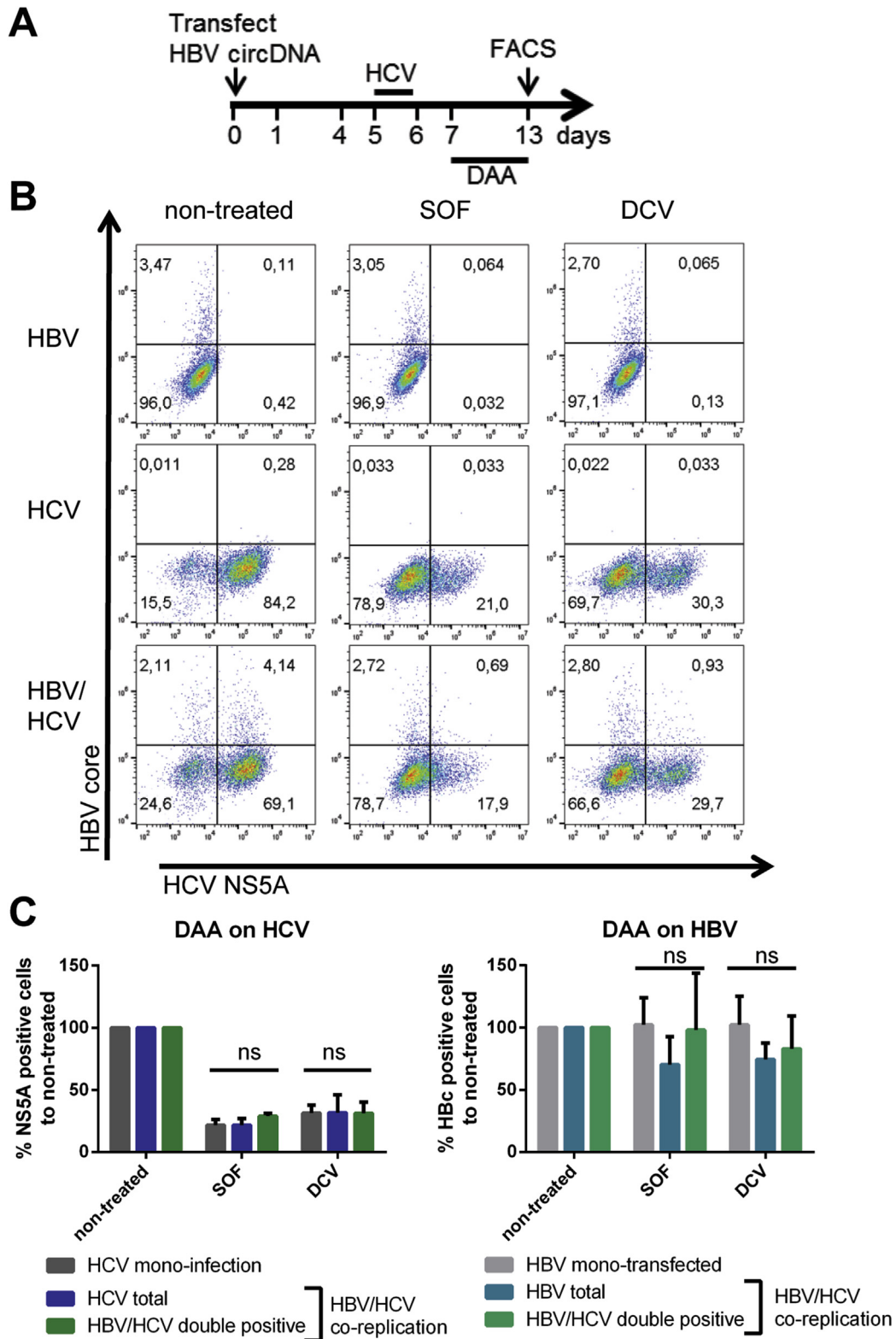
**B**



**Supplementary Figure 15.** Determination of the biological activity of IFN- $\alpha$  and IFN- $\lambda$  and antiviral effects of IFN- $\lambda$  in the HBV/HCV coreplication cell culture system. (A) Antiviral activity of IFN- $\alpha$  and IFN- $\lambda$  as determined with Huh7 cells containing a stably replicating subgenomic HCV luciferase replicon (shown in the top panel). Concentrations for IFN- $\alpha$  are given in IU/mL and for IFN- $\lambda$  in ng/mL. Calculated EC<sub>50</sub> values are 3.2 IU/mL for IFN- $\alpha$  and 0.17 ng/mL for IFN- $\lambda$ . Luciferase activity expressed from the HCV replicon was measured 72 hours after IFN treatment. (B) Representative flow cytometry panels of Huh7.5 cells superinfected with HCV (multiplicity of infection = 0.1) 4 days post transfection with cirrHBV DNA. Samples were either treated 24 hours before superinfection with HCV ("pre"-treated) or 24 hours after HCV infection ("post"-treated) or left untreated (nontreated). IFN- $\lambda$  (10 ng/mL) was added after each medium change.



**Supplementary Figure 16.** HBV inoculum does not interfere with RIG-I, MDA5, or TLR-mediated IFN induction. dHepaRG<sup>NTCP</sup> cells were inoculated with HBV (100 GE/cell), HBV + Myrcludex B (MyrB), or with medium containing 4% PEG (noninfected [NI]) as in the other inoculation conditions. After 24 hours, medium was removed, and cells stimulated for 8 hours with 20x EC<sub>50</sub> RVFVΔNSs (left panel), Mengo<sup>Zn</sup> virus (multiplicity of infection = 10) (middle panel), or 10 μg/mL poly(I:C) added into the culture supernatant (right panel). mRNA levels of IFN-β, IFN-λ, IFIT1, and GBP1 were analyzed by reverse-transcriptase qPCR. mRNA levels of IFNs were not detectable in the nonstimulated control and therefore normalized to the NI stimulated control. mRNA levels of IFIT1 and GBP1 were first normalized to the nonstimulated control of the same condition (HBV, MyrB, or NI) and then compared with the NI stimulated control. n = 2.



**Supplementary Figure 17.** DAA-mediated suppression of HCV does not impact HBV replication. (A) Schematic overview of the experimental setup. Huh7.5 cells were transfected with HBV circDNA and superinfected with HCV (multiplicity of infection = 0.1) 4 days later. Samples were treated 48 hours post HCV infection for 6 days with Sofosbuvir (SOF; 727 nM), Daclatasvir (DCV; 730 nM), or left untreated. Cells were stained for HCV NS5A and HBV core and analyzed by flow cytometry (B). A representative panel is shown. (C) Left panel: Quantification of HCV NS5A. Gray bar, cells infected only with HCV; blue bar, all cells infected with HCV; green bar, HCV/HBV coinfecting cells. Right panel: Quantification of HBV core. Color coding of bars analogous to the left panel. n = 2.

**Supplementary Table 1.** Primary Antibodies Used for Immunofluorescence and Flow Cytometry

Antigen	Species	Origin	Dilution	
			Immunofluorescence	Flow cytometry
HBV core	Chicken	Self-made	1:4000	1:200 <sup>a</sup>
HBV core	Rabbit	B0586; Dako, Glostrup, Denmark		1:750
HBV HBsAg	Human	Humabs Biomed SA, Bellinzona, Switzerland	1:3000	
HCV NS5A	Mouse	9E10; gift by Charles Rice, New York		1:2000
Mx1	Mouse	Gift by Georg Kochs, Freiburg, Germany	1:500	1:500
NF- $\kappa$ B	Mouse	L8F6, #6956, Cell Signaling, Danvers, MA	1:800	
pSTAT (pY701)	Mouse	BD #612232, BD Bioscience, San Jose, CA	1:200	

<sup>a</sup>Antibody was coupled to Alexa-647.

**Supplementary Table 2.** Secondary Antibodies Used for Immunofluorescence and Flow Cytometry

Antibody	Raised against	Origin
647-goat	Mouse IgG	Life Technologies, Carlsbad, CA; A31571
568-goat	Mouse IgG	Life Technologies; A10037
488-goat	Mouse IgG	Life Technologies; A11029
568-goat	Rabbit IgG	Life Technologies; A11036
488-goat	Rabbit IgG	Life Technologies; A11008
647-goat	Chicken IgY	Abcam, Cambridge, UK; ab150171
488-goat	Chicken IgY	Abcam; ab150173
555-goat	Human IgG	Life Technologies; A-21433 1

Ig, immunoglobulin.

**Supplementary Table 3.** DNA Oligonucleotides and Probes Used for qPCR and Taqman

Name	Sequence 5'-3'
APOBEC3A fwd	GAGAAGGGACAAGCACATGG
APOBEC3A rev	TGGATCCATCAAGTGTCTGG
APOBEC3B fwd	GACCCTTTGGTCCTTCGAC
APOBEC3B rev	GCACAGCCCCAGGAGAAG
APOBEC3G fwd	CCGAGGACCCGAAGGTTAC
APOBEC3G rev	TCCAACAGTGCTGAAATTCG
GAPDH fwd	GAAGGTGAAGGTCGGAGTC
GAPDH rev	GAAGATGGTGATGGGATTTTC
IFIT1 fwd	GAAGCAGGCAATCACAGAAA
IFIT1 rev	TGAAACCGACCATAGTGGAA
IFN- $\beta$ fwd	CGCCGCATTGACCATCTA
IFN- $\beta$ rev	GACATTAGCCAGGAGGTTCTC
IFN- $\lambda$ fwd	GCAGGTTCAAATCTCTGTCCACC
IFN- $\lambda$ rev	AAGACAGGAGAGCTGCAACTC
cccDNA fwd	GTGGTTATCCTGCGTTGAT
cccDNA rev	GAGCTGAGGCGGTATCT
cccDNA probe	FAM-AGTTGGCGAGAAAAGTGAA AGCCTGC-TAMRA
pgRNA fwd	GAGTGTGGATTTCGCACTCC-3'
pgRNA rev	GAGGCGAGGGAGTTCTTCT3
PML fwd	CGCCCTGGATAACGCTTTTTT
PML rev	CTCGCACTCAAAGCACCAGA
GBP1 fwd	ACAGAAGTGCTAGAAGCCAGTGC
GBP1 rev	TCCAGGCTGTTCCCTTGTCTGTTT
DNMT3A fwd	TATTGATGAGCGCACAAAGAGAGC
DNMT3A rev	GGGTGTTCCAGGGTAACATTGAG
IL-6 fwd	ACTCACCTCTTCAGAACGAATTG
IL-6 rev	CCATCTTTGGAAGGTTGAGTTG
STAT2 fwd	GAGCCAGCAACATGAGATTGA
STAT2 rev	GCCTGGATCTTATATCGGAAGCA
TLR3 fwd	TTGCCTTGTATCTACTTTTGGGG
TLR3 rev	TCAACACTGTTATGTTTGTGGGT

Fwd, forward; rev, reverse.